AN ABSTRACT OF THE PAPER OF

Jerome Peter Sedlak for the degree of Master of Forestry

in Forest Engineering presented on March 9, 1978

Title: The Loading of Second-Growth Douglas-fir (Pseudotsuga menziesii (Mirb.) Franco) to Simulate the Forces Acting On an Intermediate Support Tree

The commercial thinning of second-growth stands in the Pacific Northwest is becoming increasingly important for satisfying the demand for timber. Cable logging will require the rigging of smaller intermediate support trees rather than those utilized on old-growth timber sales. This paper reports on the results of a study designed to evaluate the ability of second-growth trees to sustain the compressive forces similar to those generated by a cable logging system.

The movements of nine trees subjected to increasing amounts of force were measured with two theodolites. The conditions of loading were similar to those imposed on intermediate support trees.

The study demonstrates that a tree will continue to move in the direction of its initial lateral movement. Once a tree is bent, the downward compressive force governs the movement of the tree.

The results from the study are compared to Euler's design formula. It is suggested that a factor of safety be applied when designing an intermediate support. Additional research is proposed by the author

to determine the forces acting on support trees during the actual yarding cycle.

The Loading of Second-Growth Douglas-fir (*Pseudotsuga menziesii* (Mirb.) Franco) to Simulate the Forces Acting On an Intermediate Support Tree

by

Jerome Peter Sedlak

A PAPER

submitted to

Oregon State University

in partial fulfillment of
the requirements for the
degree of

Master of Forestry

Completed (March 9, 1978)

Commencement June 1978

APPROVED:

Penn A. Peters
Associate Professor of Forest Engineering

George W. Brown
Head of Department of Forest Engineering

Date paper is presented March 9, 1978

Typed by Maja Laird for Jerome P. Sedlak

ACKNOWLEDGEMENTS

To my wife Jody, goes my heartfelt appreciation for her devotion and support during my graduate studies at Oregon State University.

I am grateful to Penn Peters, my major professor, for providing the guidance and the criticism necessary to complete this project. To Ed Aulerich and Dennis Dykstra, members of my graduate committee, I extend many thanks for their patience and expertise in reviewing the paper.

Mark Rowley and Keith Barnhart of Tree Farm Stewards and Dick Brantigan are the men responsible for the safe and efficient execution of the experiment.

Finally, I wish to thank the graduate students in the logging engineering program for the times spent away from the books.

TABLE OF CONTENTS

ENGLISH - SI CONVERSIONS

1 inch (in.) = 2.5400 centimeters (cm.)

1 foot (ft.) = 0.3048 meters (m.)

1 pound (force)(lb.) = 4.4482 newtons (N)

1 pound (mass)(lbm.) = 0.4536 kilograms (kg.)

LIST OF SYMBOLS

Symbol		Units
B1	Cable near the pull-down block	—
B2	Cable near the block in the test tree	—
B3	Cable near the load cell and tailhold	—
CØ	Slope distance between T1 and T2	feet
L	Height above ground of the choker in the test tree	feet
S1	Angle of the cable from B3 to B2	degrees
S2	Angle of the cable from B1 to B2	degrees
T1	Primary theodolite; origin of the coordinate system	—
T2	Secondary theodolite	—
T31	Observation tack at L	—
T32	Observation tack at 3/4 L	—
T33	Observation tack at 1/2 L	—
T34	Observation tack at 1/4 L	—
T35	Observation tack near the base of the test tree	—
WØ	Cable tension at the tightening	pounds

LIST OF FIGURES

LIST OF TABLES

INTRODUCTION

As the supply of old-growth timber in the Pacific Northwest dwindles, loggers will increase the volume cut from second-growth stands to meet the demand for wood. The Forest Engineering Department at Oregon State University, Corvallis, Oregon has been studying the problems associated with smallwood harvesting (2) and this project is part of that research.

Many foresters, managing forests to maximize the fiber yield, look favorably upon thinning operations in young stands. To cable log this second-growth timber, especially a thinning side, will require the rigging of trees smaller than those used in the past. To harvest the steep, broken terrain of the Northwest, loggers may increase their use of the multispan skyline system. An advantage of this system is that as the span lengths are shortened, greater deflection is achieved, reducing the skyline forces for a given payload. The employment of this system requires the rigging of trees for intermediate supports.

When using these smaller second-growth trees for intermediate supports, the rigging crew should have some knowledge of the trees' ability to withstand the compressive loads present in the system. One method of rigging an intermediate support is shown (Figure 1). With the implied geometry, the compressive load, P_C, on the right support tree will be (3):

$$P_C = T_C * \sin(A1) + T_C * \sin(A2) \quad \text{or}$$

$$P_C = T_C (\sin(A1) + \sin(A2))$$

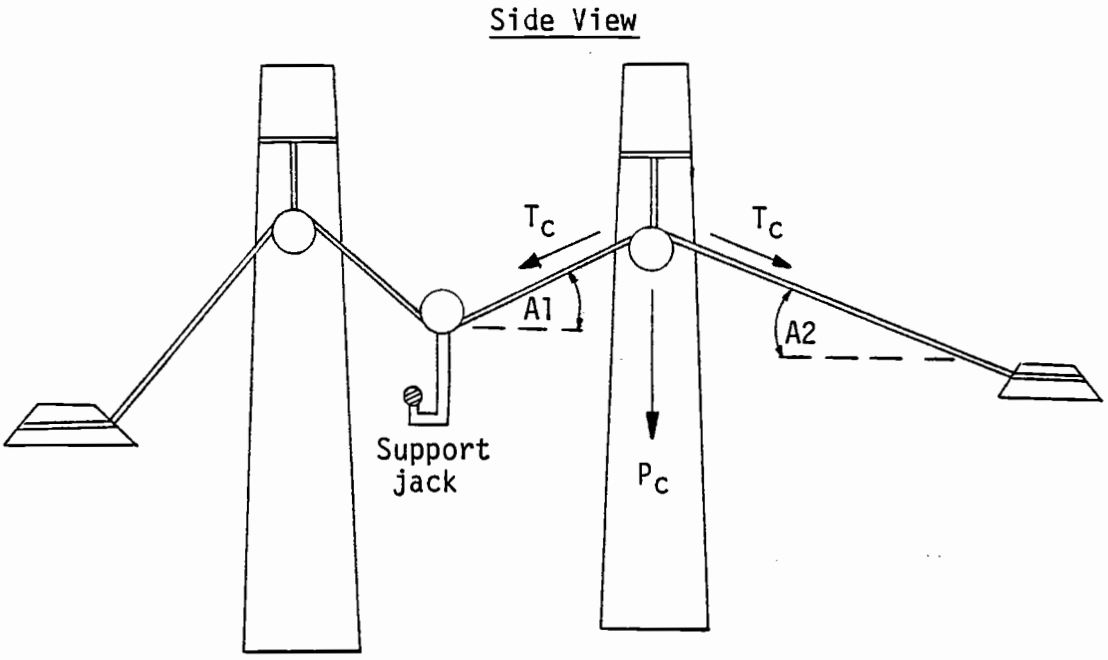

T_c = tension (lbs.) in the support cable

P_c = compressive load (lbs.) on the support tree

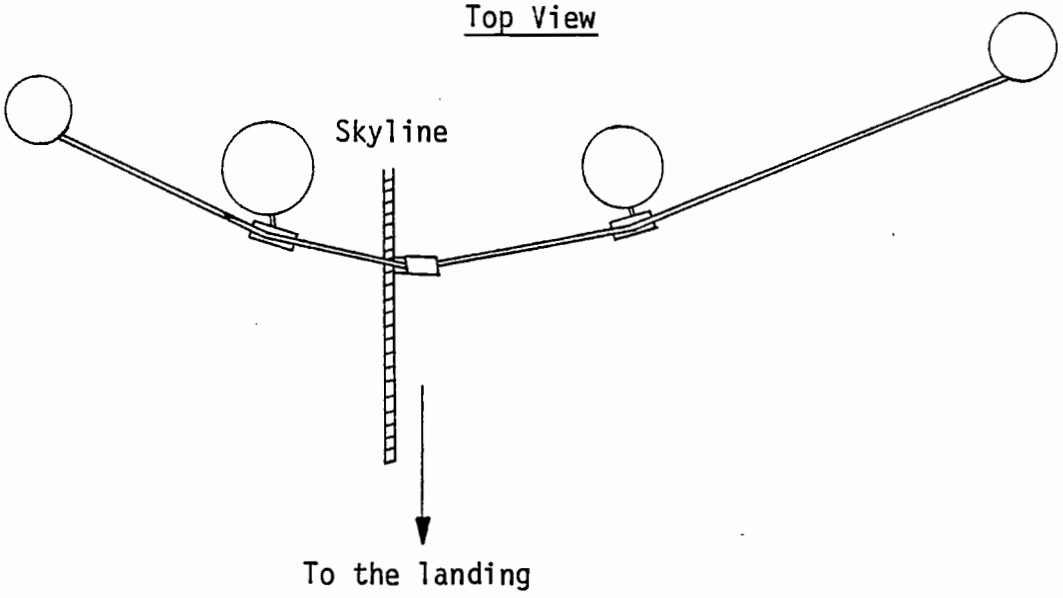

Figure 1. Method for rigging an intermediate support.

A logger must determine whether a support tree is stout enough to withstand the loads developed in a cable system, either by drawing on his past experience, looking at a table of required tree diameters, or using accepted design formulas. The experienced cable logger can decide when a tree will require buckle guys to prevent a buckling failure during the yarding operation. Often these guylines may be required by law for safety reasons and they will be rigged even though there is no danger of a tree's buckling. The rigging of unnecessary guylines can become costly in thinning operations where skyline road changes are frequent and the volume per skyline road is low.

Ernst Pestal (20,24) developed a table of required mean diameters for intermediate support trees being rigged at various heights and supporting different loads. The tabular values were valid, assuming the tree did not taper excessively. The calculations included a safety factor of five, and the supports had to be guyed sufficiently to prevent movement at the top. To Pestal's knowledge, no support tree had broken if it had been selected using his table.

Donald Biggs (4,5) realized that the maximum permissible load that can be applied to a long wood member will depend upon the length to diameter ratio, the end fixing conditions, and the species of the tree. A formula, obtained by modifying Euler's buckling formula, was used to compute the maximum load before buckling occurs. The following formula used for pine, spruce, and similar species was considered valid when the length/diameter ratio of the tree was greater than five. The tree would be considered a long column.

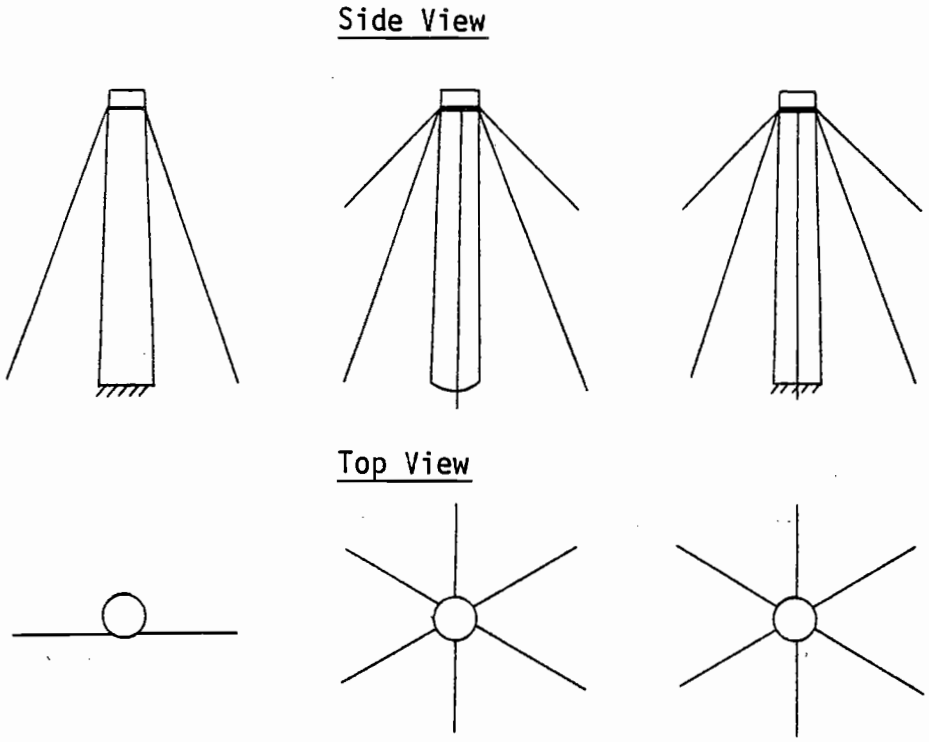

Figure 2. End-fixing constants.

$$P = \frac{1533\ D^2}{1 + (0.0213\ a\ \frac{L^2}{D^2})}$$

P = maximum compressive load (lbs.)

L = height (in.) above ground of the applied load

D = mean diameter (in.) inside bark (i.b.)

a = end-fixing constant (Figure 2)

When a rooted tree is used as a support and the top is unrestrained in one direction, and where bowing can be expected because the tree is not restrained parallel to the skyline, "a" equals 4.00. For a well-

guyed raised tree, "a" equals 1.00. If the top of a rooted tree is guyed sufficiently, then "a" equals 0.44.

The common equation used in determining the failure compressive loading is the one developed by Euler (15,21). The general equation for the critical load causing buckling of tapered, circular cross-section, long columns is:

$$P_{cr} = \frac{K \pi^3 E D^4}{64 L^2}$$

P_{cr} = compressive load (lbs.) at failure

L = height (in.) above ground of the applied load

D = diameter (in.), (i.b.) at 2L/3

E = modulus of elasticity, pounds per square inch (p.s.i.). E for West Coast Douglas-fir was assumed to be 1,600,000 p.s.i.

π = 3.1416

K = end-fixing constant (Figure 2)

Experiments have been conducted in laboratories to determine the compressive strength of different lumber grades (1,15,18). Field tests have examined a tree's resistance to lateral forces (4,8,22), but compressive loading in the woods has not been studied. This project studies the behavior of the second-growth Douglas-fir when subjected to compressive loadings similar to those encountered in cable logging operations.

OBJECTIVES

The specific objectives of the project are:

1. To study the ability of rooted second-growth Douglas-fir (*Pseudotsuga menziesii* (Mirb.) Franco) to sustain compressive loads similar to those imposed on intermediate support trees.
2. To measure the movement of the trees when subjected to these loads.
3. To present the data obtained in sufficient detail for it to be used in future, more detailed analytical studies.
4. To compare the test results at failure with Euler's design formula.

PROCEDURE

The site chosen for the experiment was located in the S.E. 1/4, S.W. 1/4, Section 35, Township 10 South, Range 5 West, Willamette Meridian. The test area was within the boundaries of the McDonald State Forest near Corvallis, Oregon (Figure 3).

The ages of the trees tested ranged from 31 to 39 years (Table 1). The site, on top of a ridge, was at an elevation of 1260 feet.

Test Tree #	Age (yrs.)
1	31
2	34
3	32
4	33
5	32
6	39
7	31
8	34
9	33

Table 1. Ages of the Nine Test Trees.

The soil was a silty clay, friable, medium acid soil (9). The depth of the surface soil ranged from 16 to 26 inches. This surface layer contained approximately 20 percent organic matter and was highly permeable. The subsoils were clays increasing in stoniness with depth. Total soil depth was approximately 40 inches. The whole soil profile

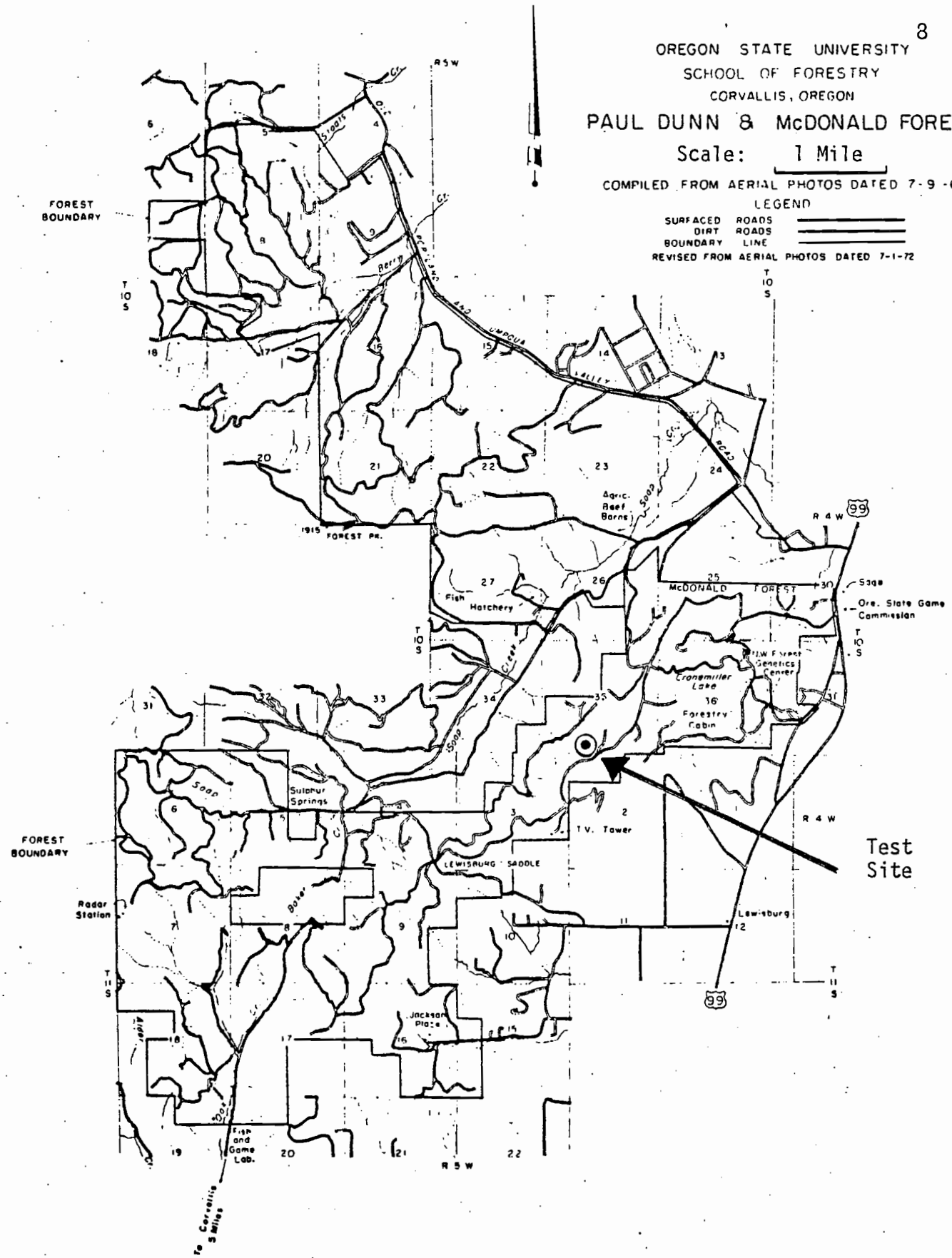

Figure 3. Map of study location.

was dark reddish brown, but it increased in clay content and acidity with depth. The soil mantle was formed over basic igneous rock.

The initial step was to locate nine appropriate trees for the experiment. Each test tree needed to be in as straight an alignment as possible with two other trees. Ideally, the test tree would be halfway between the other two. One tree would be used as a tailhold (B3) while the other would hold a pull-down block (B1) (Figures 4,5). The reason for this alignment was to minimize the lateral forces acting on the test tree.

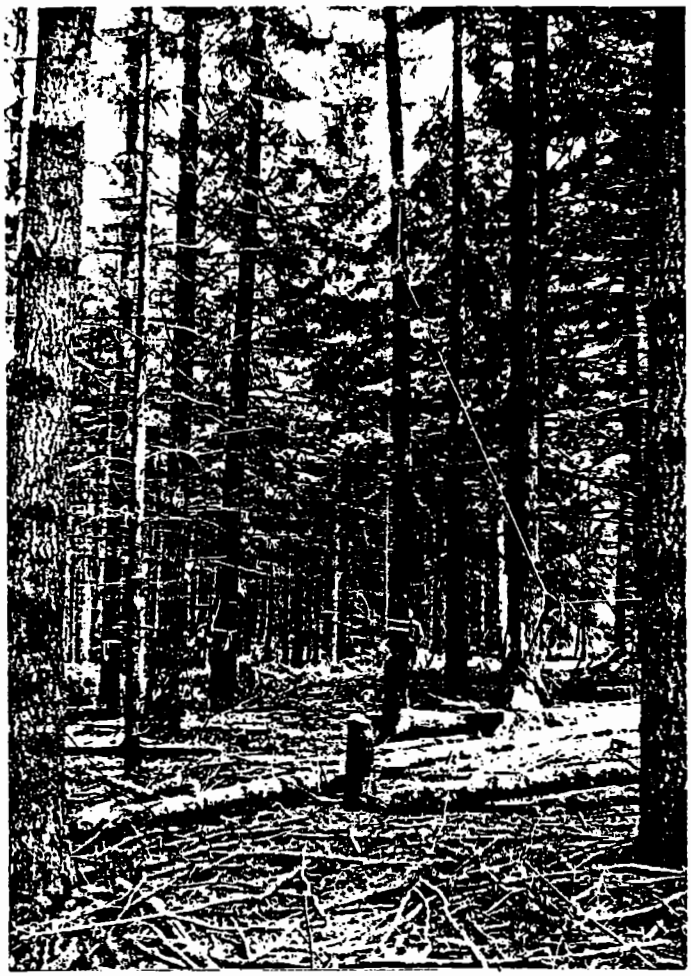

Figure 4. Cable and blocks for test tree #8, loading #1.

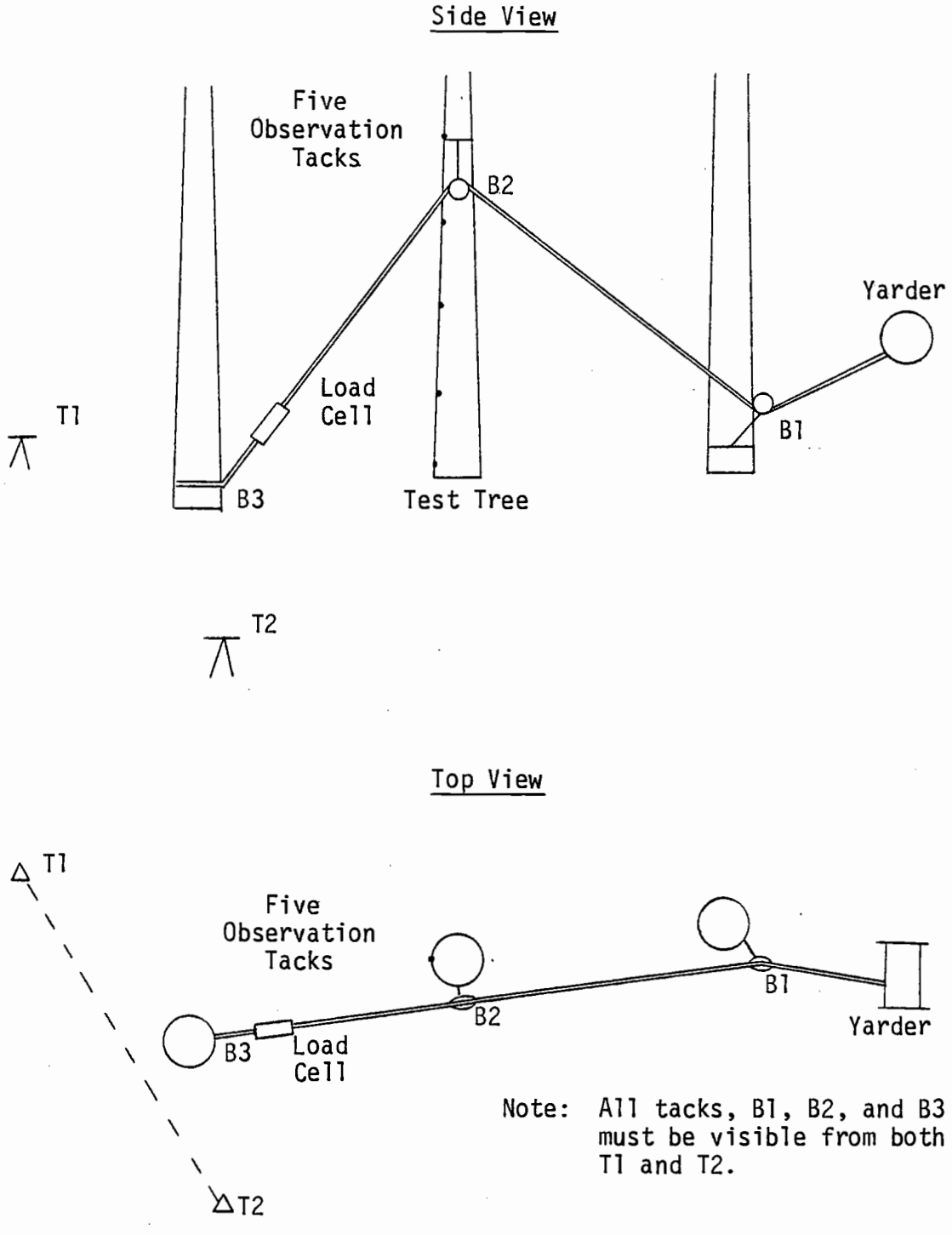

Figure 5. Experimental set-up.

Seven trees were to be rigged at a choker height (L) of 40 ft., and the diameters, outside bark (o.b.), at the choker would range from 5 to 11 inches. The other two trees were to be rigged at different heights. The diameter, o.b., at 2L/3 of these two trees had to equal the diameter o.b. at 26.7 ft. (2/3 of 40 ft.) of one of the other seven trees. This was done to examine the effect of different rigging heights in trees with the same diameter at 2L/3. Theoretically, the compressive forces required to break these trees would be proportional to the inverse of the rigging heights squared (15).

As each tree was selected, positions for the two theodolites, T1 and T2, were staked. From each position, the instrument man had to have an unobstructed view of B1, B3, the block in the tree (B2), and the test tree's stem. This often necessitated limbing the surrounding trees.

Every test tree was limbed to the desired height, measured with a 200-ft. steel tape. Using a Lietz T60-D theodolite and the steel tape, the crew set observation tacks along the stem (Figure 6). Diameters o.b., at 5-ft. intervals and at each observation tack along the stem were recorded (Table 2).

This preliminary work took two men four days to complete. All was finished before the yarder was moved to the test site.

The yarder employed for the experiment was a Schield-Bantam T-350 rubbermounted three-drum mobile yarder (Figure 7). The mainline drum with a 3/4 in. wire rope did the pulling. The line was pulled off the drum, placed in the block at B1, lifted to the block at B2, and

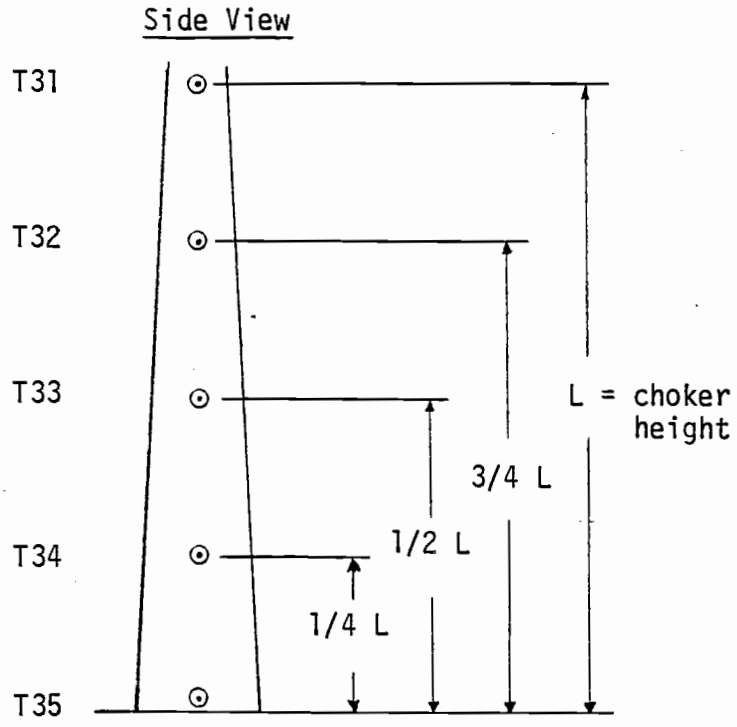

Note: T35 not at ground level so that it can be seen from T1 and T2.

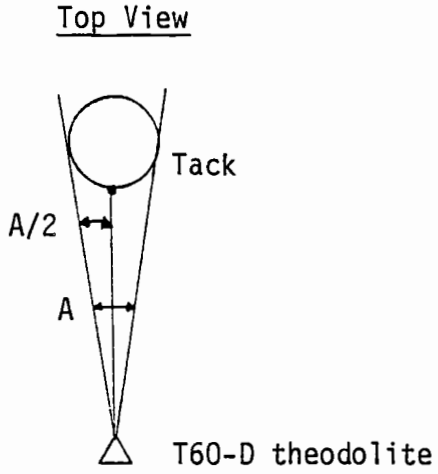

Note: Angle A was determined for each tack along the stem of the tree.

Figure 6. Placement of the observation tacks.

Observation Tack	Height Above Ground (ft.)	Test Tree 1	2	3	4	5	6	7	Height Above Ground (ft.)	Test Tree 8	Height Above Ground (ft.)	Test Tree 9
T31	40.0	8.1	5.8	9.5	9.9	7.8	7.0	10.4	24.0	8.5	47.3	7.4
											45.0	7.6
	35.0	8.4	6.4	9.8	11.1	8.4	7.3	11.0	20.0	8.9	40.0	8.2
T32	30.0	8.8	6.7	10.2	11.3	8.8	7.8	12.0	18.0	8.9	35.4	8.8
											35.0	9.3
2L/3	26.7	9.2	7.0	10.5	11.5	9.2	8.2	12.1	16.0	9.2	31.5	9.2
	25.0	9.6	7.5	10.8	12.0	9.3	8.1	12.3	15.0	9.2	30.0	9.5
											25.0	9.9
T33	20.0	9.8	7.5	11.5	12.8	9.7	8.7	12.8	12.0	9.4	23.6	10.2
									10.0	9.5	20.0	10.8
	15.0	10.1	7.9	11.5	13.1	10.2	8.7	13.0			15.0	10.8
T34	10.0	10.7	8.2	12.0	13.7	10.4	9.0	13.5	6.0	10.4	11.8	11.0
											10.0	11.1
	5.0	11.6	8.5	13.0	15.2	11.0	9.5	14.8	5.0	10.4	5.0	11.4
T35		15.0	12.1	15.5	19.1	15.3	13.7	21.1	0.54	13.9	0.26	14.7
	*height	0.96'	0.64'	0.78'	0.94'	0.52'	0.26'	0.57'				

*Height above ground for T35 is different for each tree.

Table 2. Diameters, In., Outside Bark Along the Stems.

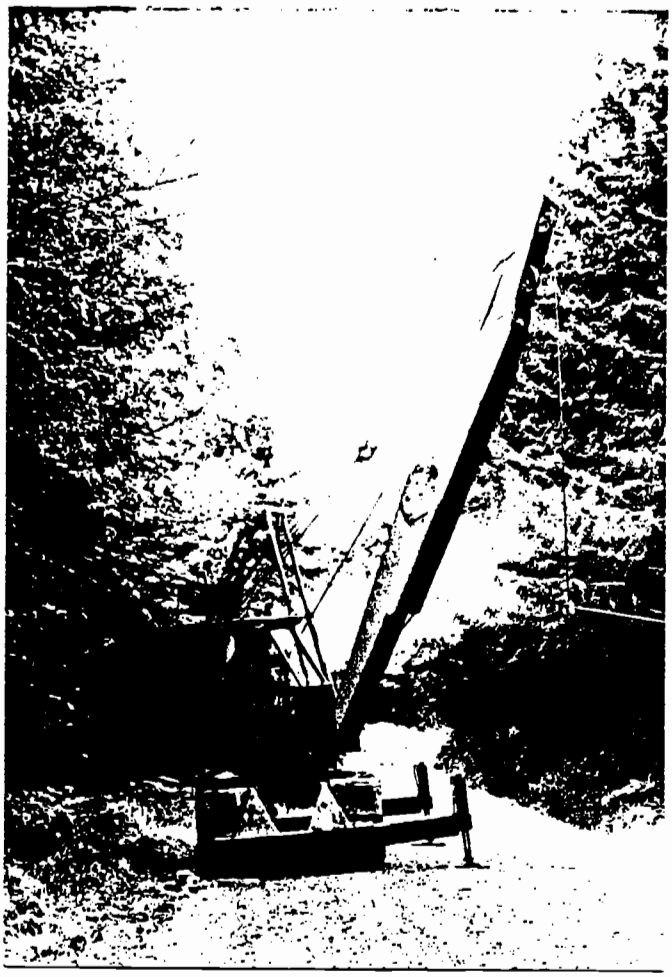

Figure 7. Schield-Bantam T-350 mobile yarder.

shackled to the load cell located near B3. The cable tensions were measured to the nearest one hundred pounds by a Dillon in-line load cell and recorded by a Rustrak strip chart recorder (Figure 8).

The yarder engineer pulled in the mainline and the cable was tightened until no slack remained. At this point the engineering crew (one man on each theodolite and one man observing the tension gauge) began their work. As the cable tightened, the man at theodolite T1 (Figure 9) recorded the horizontal and vertical angles, to the nearest one-half minute, from T1 to B1, B2, B3, and the five observation tacks.

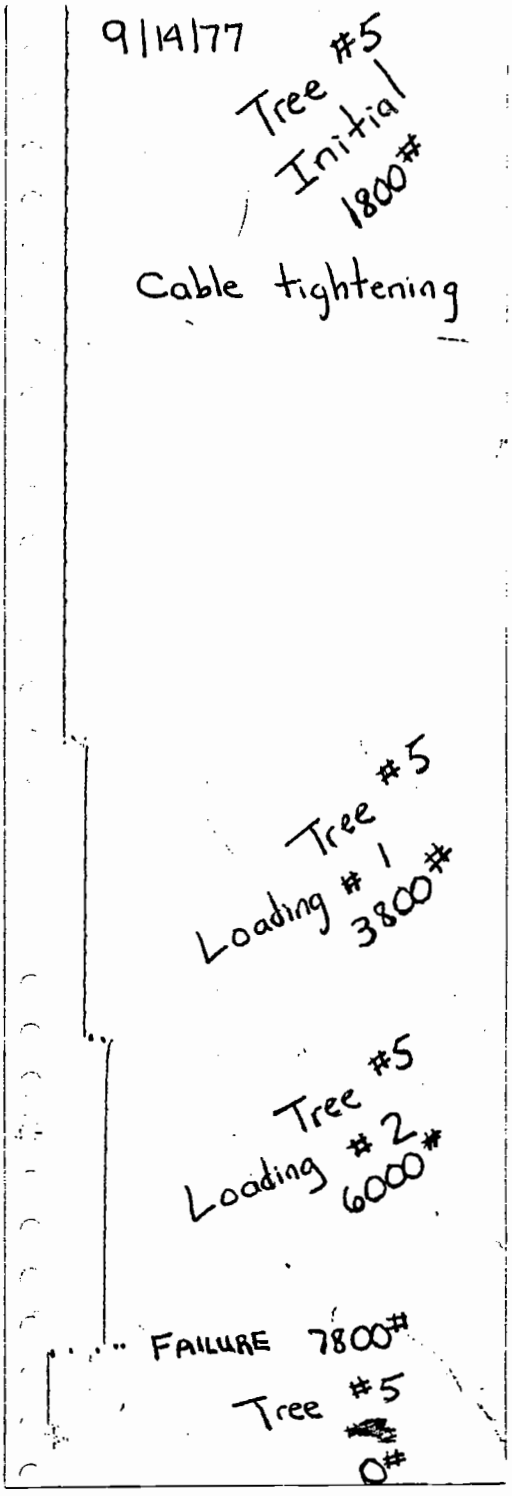

Figure 8. Strip chart record for test tree #5.

Figure 9. The author at theodolite T1 for test tree #8.

At a horizontal distance of 50 ft., a $0^{o}00'30"$ angle subtended a chord of 0.007 ft. The man at T2 recorded the horizontal angles from T2 to the same points. The vertical angle (VØ) and the slope distance (CØ) from T1 to T2 were recorded (Appendix A, Figure 35). These measurements were needed to establish a coordinate system and to calculate the coordinates of each point (Appendix A, Figures 36, 37). A clinometer was used to measure the angle along the cable from B3 to B2 (S1) and the angle along the cable from B1 to B2 (S2). These measured angles were used as a check on the calculation of the cable angles (Appendix A, Figure 38). The cable tension for the cable tightening (WØ) was also recorded.

The tension in the cable was increased in various loading increments (Table 3) until the tree broke. The yarder engineer was signaled to

Loading	Test Tree #								
	1	2	3	4	5	6	7	8	9
Tightening	1000	300	900	1700	1800	1100	400	1900	900
1	1700	1100	2800	4800	3800	2200	3300	5600	2100
2	2700	2100	4500	6600	6000	3500	6100	9000	3100
3	3000	3200	5000	8500	—	4600	6800	11,200	5500
4	3500	1200[a]	5200	11,900	—	2700[d]	—	—	7400
5	3900	—	4900[b]	13,000	—	2500[d]	—	—	—
6	—	—	—	14,000	—	—	—	—	—
7	—	—	—	15,700	—	—	—	—	—
8	—	—	—	8000[c]	—	—	—	—	—
9	—	—	—	12,000	—	—	—	—	—
10	—	—	—	13,900	—	—	—	—	—
11	—	—	—	2000[c]	—	—	—	—	—
12	—	—	—	5900	—	—	—	—	—
13	—	—	—	9500	—	—	—	—	—
Failure	5500	1800	6900[b]	11,500	7800	3000	7100	14,300	9200

[a] Top of the test tree broke at the choker.

[b] Failure tension was achieved between loadings #4 and #5. Tree #3 broke while holding 4900 lbs. at loading #5.

[c] Change location of the blocks.

[d] Limbs breaking in the top of the test tree and in adjacent trees.

Table 3. Cable Tensions (lbs.).

Figure 10. Test tree #3 being held stationary at loading #4.

hold the tension constant after each increment (Figure 10). He accomplished this by braking the drum and then shutting off the yarder.

For the first two trees tested, #1 and #3, the crew recorded the movements of T31, T33 and B2. At each loading increment, the horizontal and vertical angles from T1 to each of these three points were recorded. The horizontal angles from T2 to T31, T33 and B2 were also noted, as was the tension in the cable. The crew assumed that B1 and B3, designated by ribbons on the cable near the pull-down block and

the load cell respectively, remained stationary. During the testing of the third tree, the strap with the pull-down block at B3 slipped. For the seven remaining trees, the position of the cable was noted by shooting the angles from T1 and T2 to B1 and B3 at each increment (Figure 11). If the ribbons on the cable were obscured by neighboring trees as the cable shortened, a crew member slid the ribbons along the cable until they could be seen from both T1 and T2.

A major deviation in the loading procedure occurred during the testing of tree #4. After seven loadings, the tree had barely moved and

Figure 11. Reading angles from T1 for test tree #5 at loading #2.

the yarder had reached its maximum pull of 16,000 pounds. To increase the compressive load, the pull-down block at B1 was lowered approximately one foot. This did not help to fail the tree during loadings #8 through #10. Before loading #11, the tailhold, B3, was moved to a maple stump 26 feet nearer the test tree. This change in block location led to the tree's failure.

After a tree failed, with the cables and the upper portion of the tree falling to the ground, the remaining stem returned to an upright position. The angles to the break and to any remaining observation tacks were recorded.

The actual loading of the trees required four days to complete during the week of September 12, 1977.

ANALYSIS

The initial step in the analysis of the field data was the calculation of the coordinates for the different points. Computer programs for the Hewlett-Packard 9830 desk top calculator were written by the author to perform this task. Each test tree had its own right-handed X, Y, Z coordinate system. The origin was the theodolite T1, and the positive X-axis was the horizontal line in the direction of T2. The horizontal Y-axis was perpendicular to this line with the test tree standing in the first quadrant. The positive Z-axis rose vertically from T1. The coordinates of the points measured during the cable tightening and the loading increments for each tree were tabulated (Appendix B, Tables 8-17).

The original and the failure coordinates of B2, T31, and T33 had to be extrapolated from graphs (Figure 12). Before proceeding with the graphical extrapolations, the author knew the coordinates for B1, B2, B3, T31, and T33 at the cable tightening and each loading. The points B1 and B3 never moved a significant amount to warrant the extrapolations to determine their original and failure positions. The crew did not realize the trees moved appreciably from their original positions during the cable tightening until the last two trees were tested. During the experiment, no angles were measured from the theodolites until after the cable tightening with the cable sufficiently taut to measure the angles S1 and S2 with a clinometer. The failure position was not recorded in the field because the tree broke after the last recorded loading increment and the stem above the break fell to the

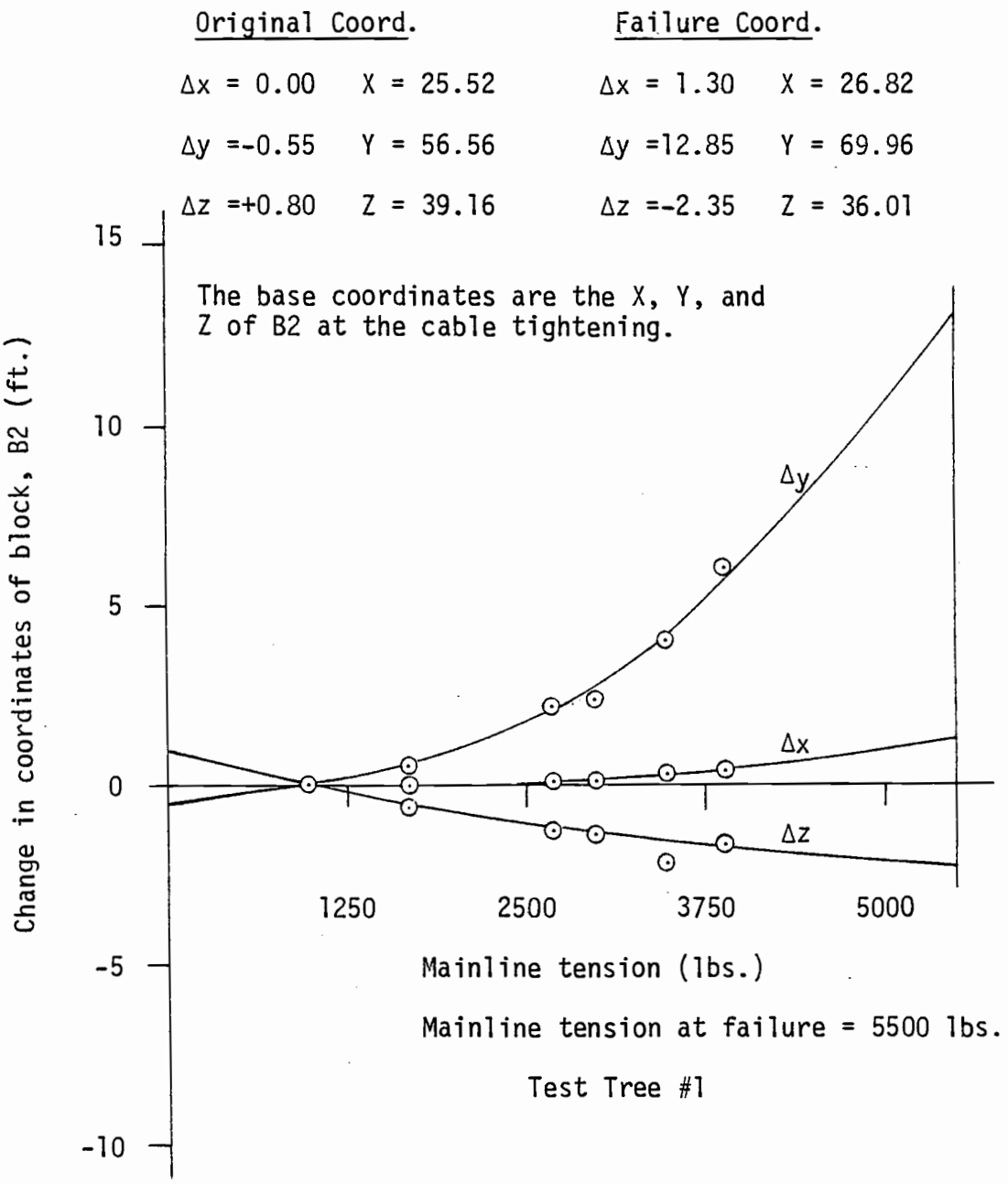

Figure 12. Extrapolation to determine the original and failure coordinates.

ground along with the block B2. The rooted stem of the test tree would return to an upright position. The mainline drum on the yarder was not sensitive enough to increase the cable tension in small, uniform amounts before failure occurred. Originally three days were budgeted for the actual testing, so the loading procedure for each tree could not take more than two or three hours. This limited time allotment was a factor in deciding how much to increase the cable tension at each loading.

Knowing the coordinates of B1, B2, and B3 and the cable tension, the author employed vector analysis to determine the forces acting on the test tree. For each loading, the unit vectors of the cable segments B3B2 and B1B2 were multiplied by the tension in the cable and the force components in the X, Y, and Z directions were summed (Appendix C, Tables 18-26). At failure, B1 and B3 were assumed to have not moved since the last loading increment. The forces calculated were acting at the block B2. The resultant force was transmitted through the 3/4-inch choker and acted on the test tree at T31.

With the X and Y coordinates plotted, the lateral movement of the test tree as the cable tension increased can be observed (Figures 13-21). The plotted points represent the location of T31 at its extrapolated original position (⊖), at the cable tightening and at each loading increment (⊙), and at the extrapolated failure position (⊗). The positive X-axis increases from the top to the bottom of each figure and the positive Y-axis is oriented from the left to the right:

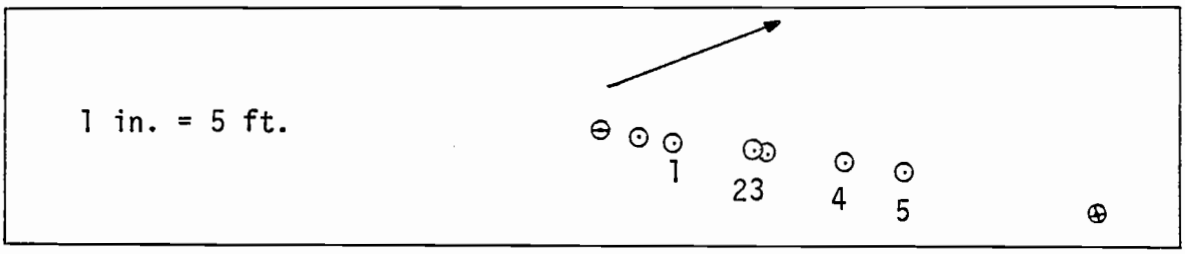

Figure 13. Lateral movement of T31 for test tree #1.

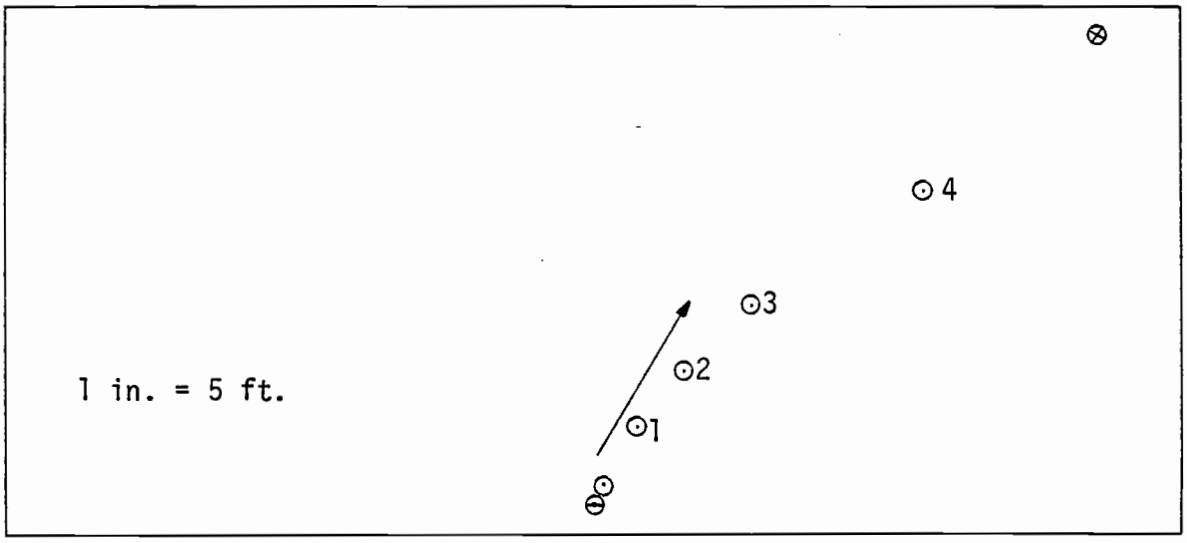

Notes: At loadings #1, #2, and #3, the test tree leans into an adjacent tree.

During loading #4, the top of the test tree breaks at choker height. There is no more resistance to lateral movement at the top. The cable tension decreases.

Figure 14. Lateral movement of T31 for test tree #2.

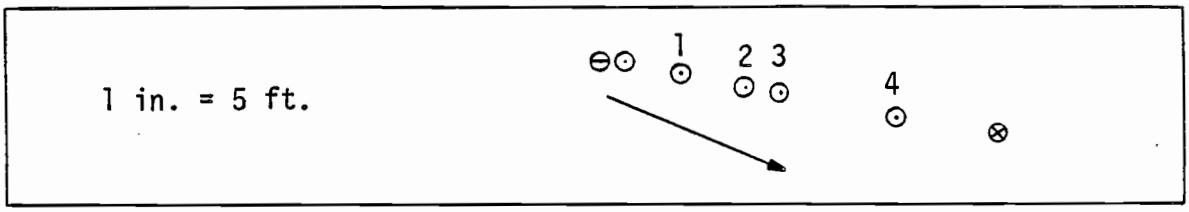

Notes: The test tree fails at a cable tension of 6900 lbs. reached between loadings #4 and #5, as the tree is pulled through adjacent tops.

The positions of T31 and T33 at loading #5 are not recorded as the tree suddenly fails before the angles to T31 and T33 can be read.

Figure 15. Lateral movement of T31 for test tree #3.

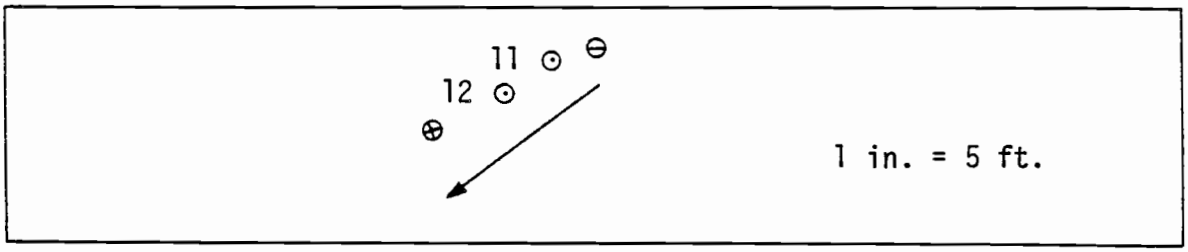

Notes: The points plotted are the original position, positions at loadings #11 and #12, and the failure position of T31.

One cannot see T31 and B2 from T1 during loading #13.

Figure 16. Lateral movement of T31 for test tree #4.

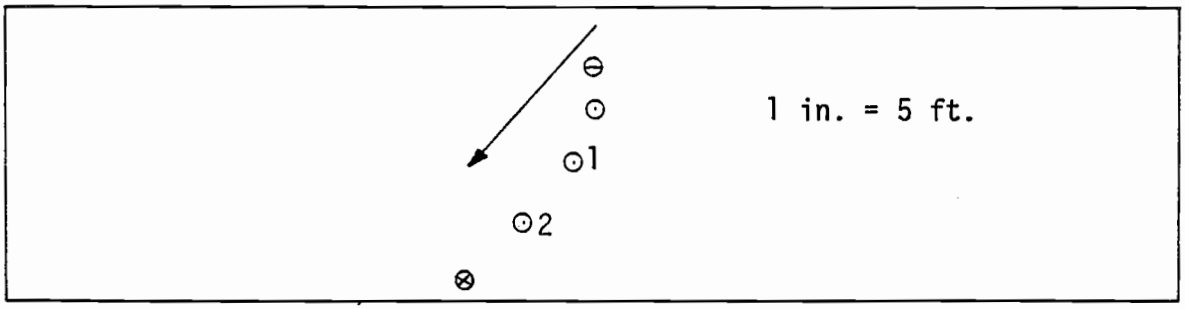

Note: At loading #2, the top of the test tree is hitting adjacent tops.

Figure 17. Lateral movement of T31 for test tree #5.

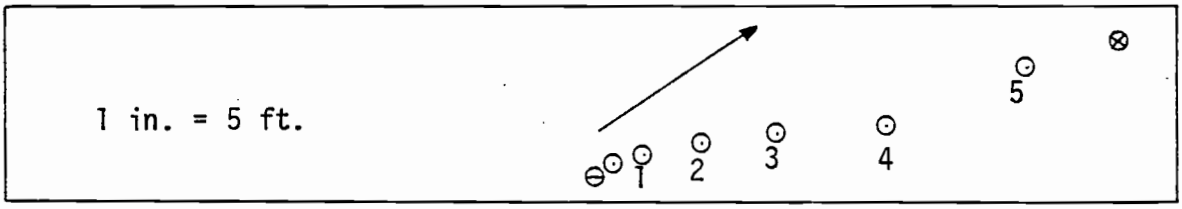

Notes: At loading #3, the top of the test tree is leaning into the branches of another tree.

During loading #4, the branches break in the tops of the test tree and the other tree. The cable tension decreases.

During loading #5, the cable tension decreases more as the test tree moves away from some adjacent tops. The tree is stopped before hitting another top.

Figure 18. Lateral movement of T31 for test tree #6.

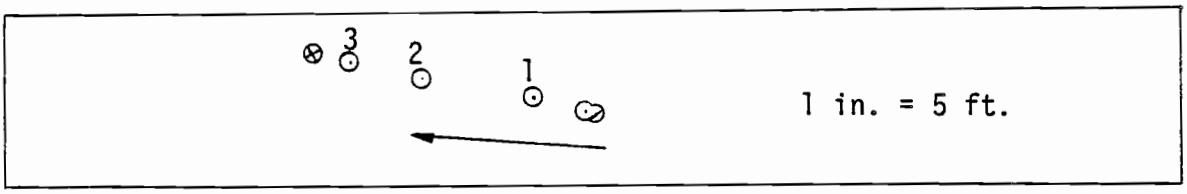

Figure 19. Lateral movement of T31 for test tree #7.

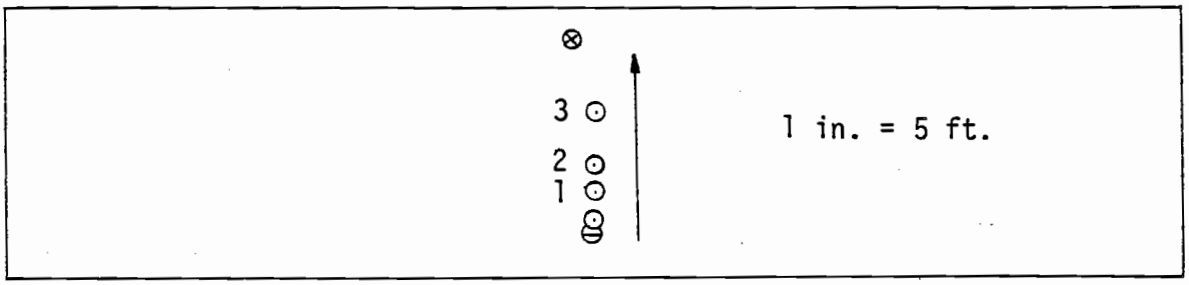

Note: At loadings #2 and #3, the top of the test tree leans into the top of the tree with the load cell.

Figure 20. Lateral movement of T31 for test tree #8.

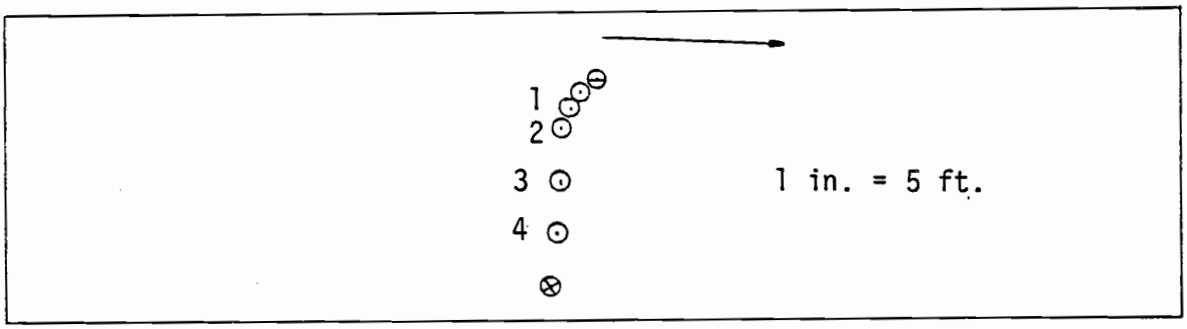

Notes: At loading #3, the top of the test tree begins to hit adjacent tops.

Test tree still hits adjacent tops during loading #4.

Figure 21. Lateral movement of T31 for test tree #9.

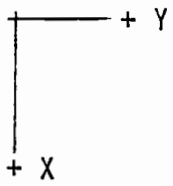

The arrow on each figure represents the direction of the lateral force (vector sum of the X and Y components) acting on the test tree at the cable tightening. It is not drawn to scale to represent the magnitude of the initial force.

The coordinates of B1, B2, and B3 were used to compute the vertical angles of cable segment B3B2 or B1B2 with respect to a horizontal plane passing through B3 or B1. These angles were determined for the cable tightening, the loading increments, and the failure position of each test tree (Appendix D, Tables 27-35). The horizontal alignment of the blocks with respect to the movement of T31 are plotted for every test tree (Figures 22-30). The cable segments are drawn for the cable tightening and the failure position. The vertical angles of the cable segments at these two positions are recorded below each figure.

After each tree failed, the rooted stem returned to an upright position. The two crew members using the theodolites agreed on a common point to shoot on the break. The height of the break above the ground and the diameter of the stem were tabulated for each tree (Table 4). The diameters at the breaks were calculated using linear interpolation between the two closest measured diameters. Trees #4 and #7, the two largest trees tested, experienced a different kind of break (Figure 31). These two breaks had distinct tops and bottoms to them, whereas each of the seven other trees failed in a single horizontal plane across the stem.

1 in. = 10 ft.

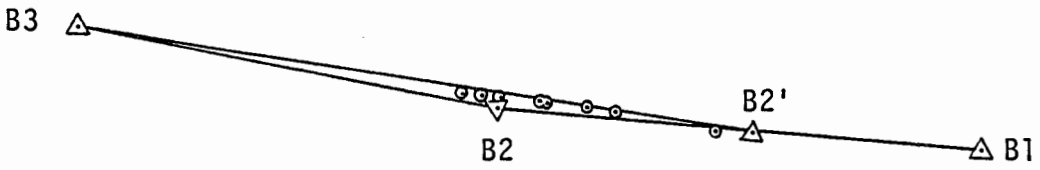

Vertical Angles

Cable Tightening	Failure Position
B3B2 - 55.9°	B3B2' - 40.7°
B1B2 - 47.6°	B1B2' - 64.4°

Figure 22. Cable alignment for test tree #1.

1 in. = 10 ft.

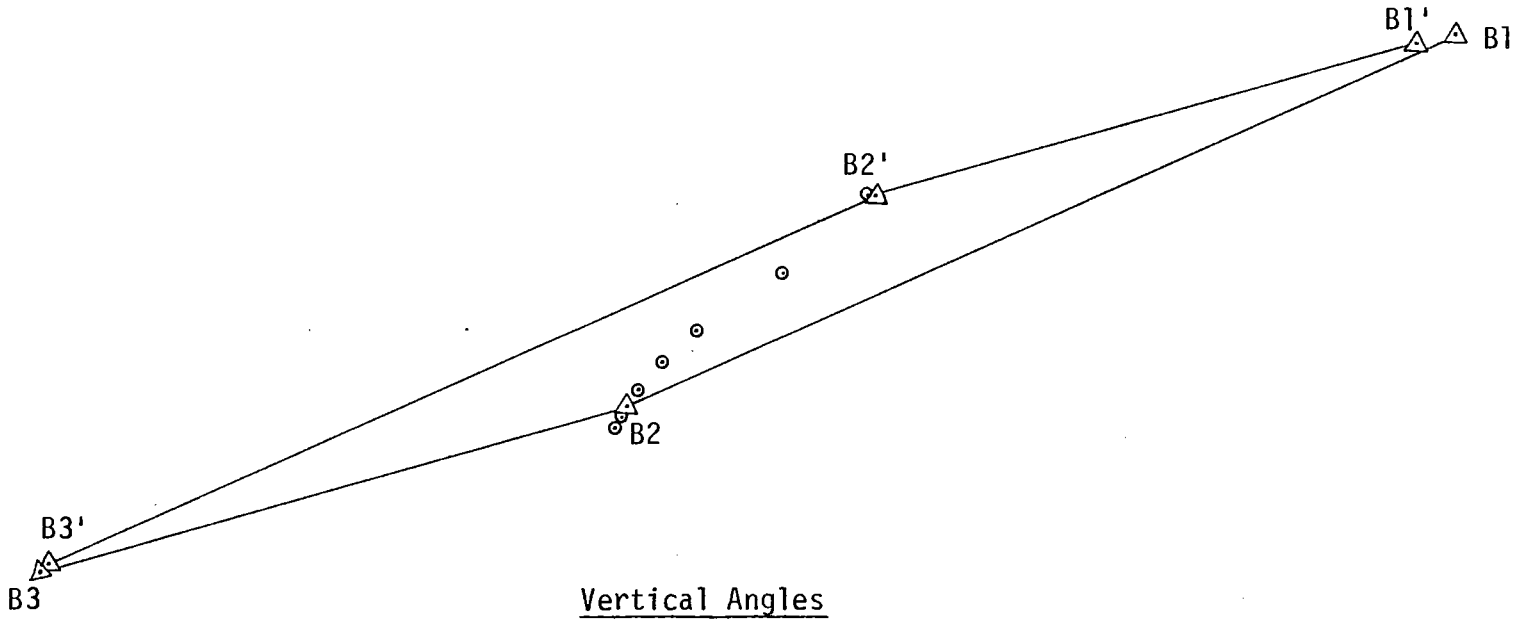

Vertical Angles

Cable Tightening	Failure Position
B3B2 - 46.4°	B3'B2' - 31.2°
B1B2 - 32.9°	B1'B2' - 38.8°

Figure 23. Cable alignment for test tree #2.

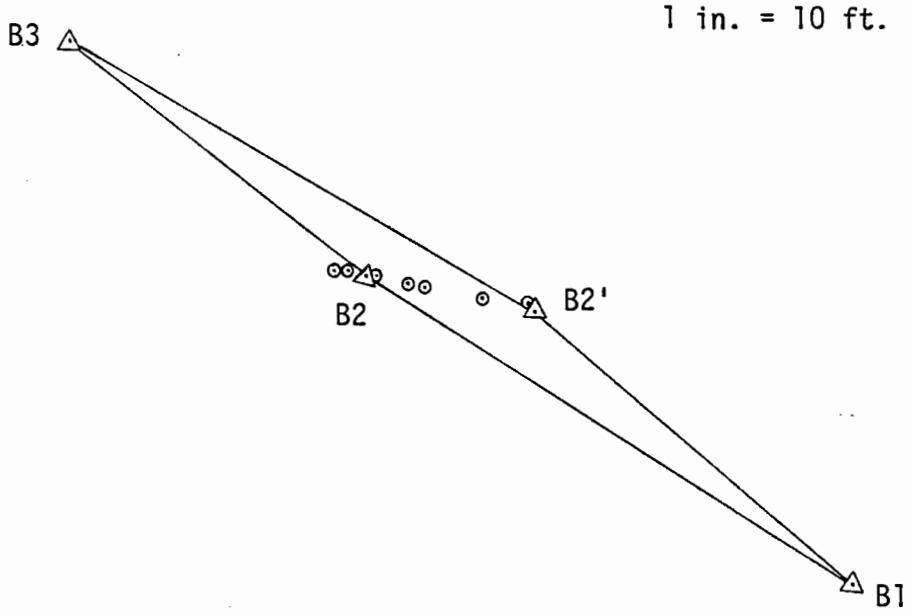

Vertical Angles

Cable Tightening	Failure Position
B3B2 - 59.5°	B3B2' - 48.6°
B1B2 - 43.4°	B1B2' - 50.5°

Figure 24. Cable alignment for test tree #3.

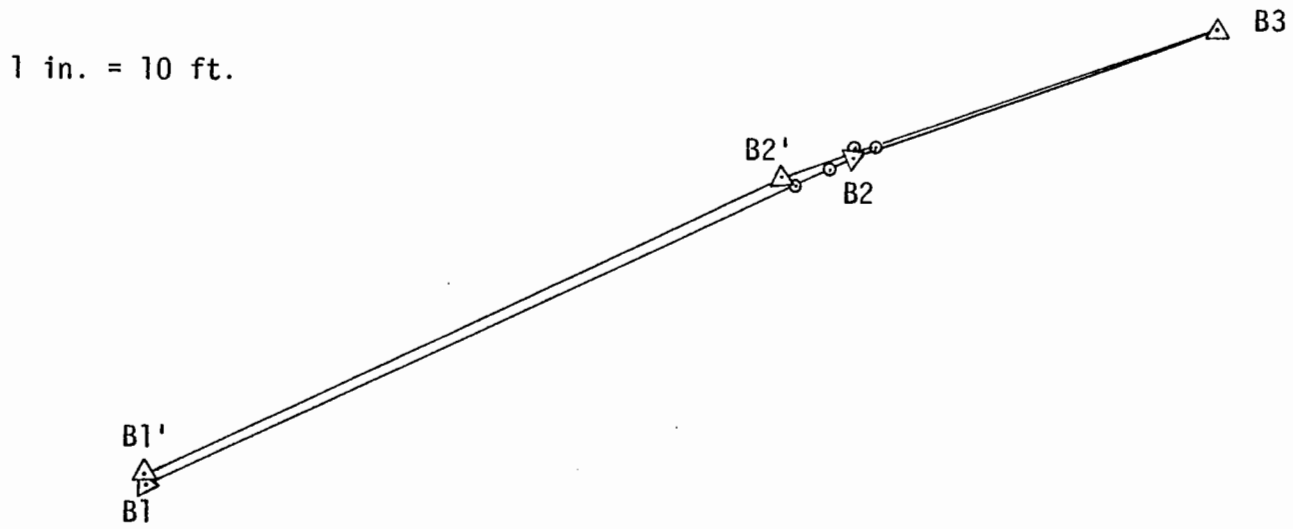

Vertical Angles

Loading #11	Failure Position
B3B2 - 56.1°	B3B2' - 50.6°
B1B2 - 37.3°	B1'B2'- 38.8°

Figure 25. Cable alignment for test tree #4.

1 in. = 10 ft.

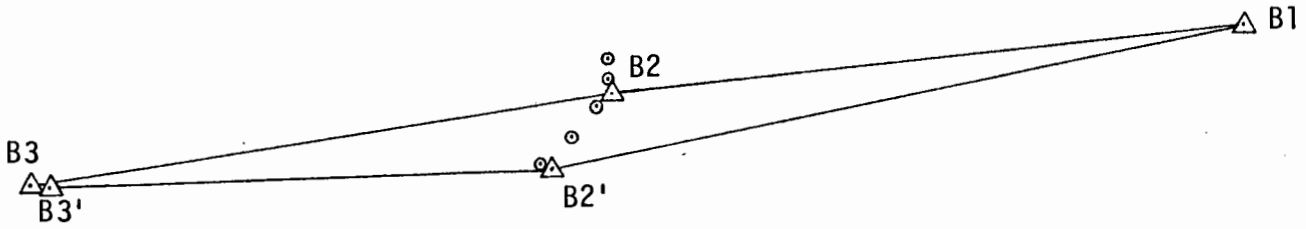

Vertical Angles

Cable Tightening	Failure Position
B3B2 - 44.6°	B3'B2' - 47.0°
B1B2 - 47.9°	B1B2' - 44.4°

Figure 26. Cable alignment for test tree #5.

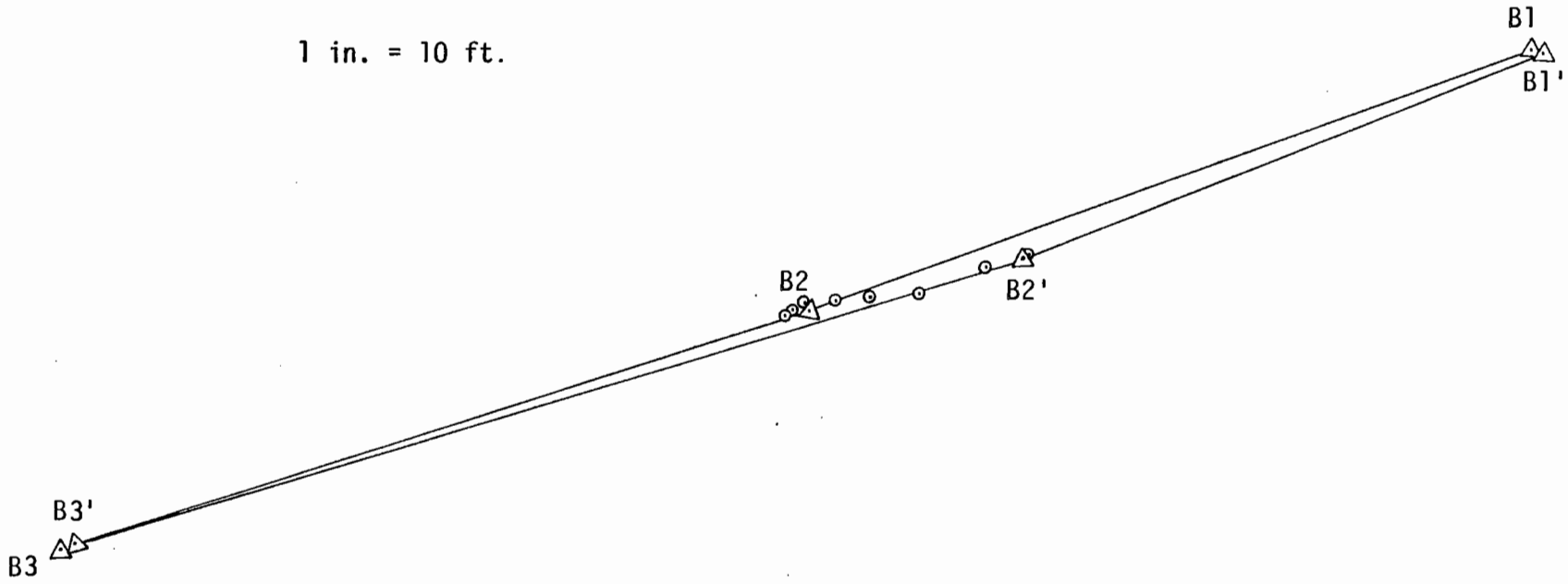

Vertical Angles

Cable Tightening	Failure Position
B3B2 - 42.6°	B3'B2' - 33.8°
B1B2 - 31.5°	B1'B2' - 36.8°

Figure 27. Cable alignment for test tree #6.

1 in. = 10 ft.

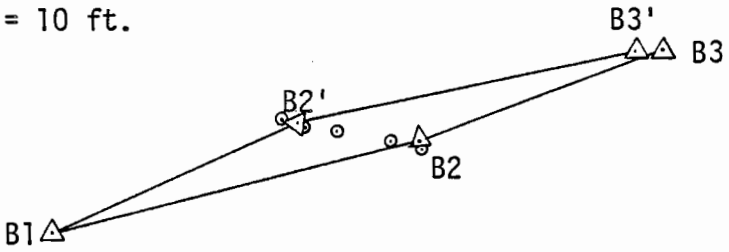

Vertical Angles

Cable Tightening	Failure Position
B3B2 - 66.5°	B3'B2' - 56.9°
B1B2 - 56.9°	B1B2' - 62.3°

Figure 28. Cable alignment for test tree #7.

1 in. = 10 ft.

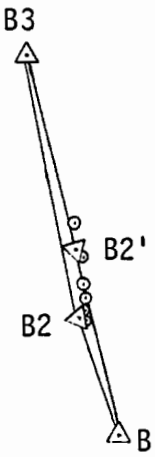

Vertical Angles

Cable Tightening	Failure Position
B3B2 - 51.6°	B3B2' - 57.2°
B1B2 - 65.8°	B1B2' - 53.9°

Figure 29. Cable alignment for test tree #8.

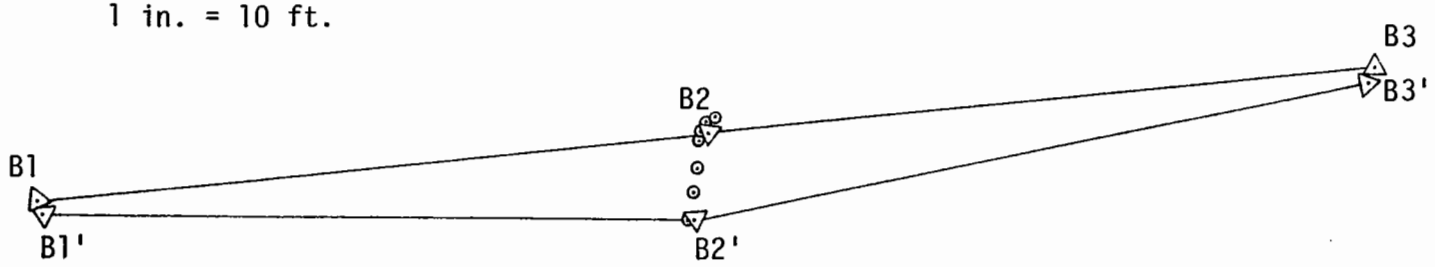

Vertical Angles

Cable Tightening	Failure Position
B3B2 - 47.3°	B3'B2' - 44.6°
B1B2 - 48.9°	B1'B2' - 48.5°

Figure 30. Cable alignment for test tree #9.

Test Tree	Height (ft.) Above Ground	Diameter (in.) Outside Bark*	Diameter (in.) Inside Bark**
1	16.75	10.0	9.3
2	20.21	7.5	7.0
3	26.60	10.5	9.8
4 Top	23.11	12.3	11.5
4 Bottom	16.09	13.0	12.1
5	20.15	9.7	9.1
6	15.79	8.7	8.1
7 Top	24.78	12.3	11.5
7 Bottom	18.28	12.9	12.0
8	9.13	9.7	9.1
9	32.44	9.4	8.8

* Determined by interpolation

** Diameter, i.b. = [(0.93)(Diameter, o.b.) + 0.04] inches, after Khan, et. al. (11)

Table 4. Heights (ft.) and Diameters (in.) of the Breaks.

Figure 31. Breaks of test trees #4 (left) and #7.

Before calculating the failure stress in the tree, the location of the break was determined from linear interpolation using the coordinates of T35 and the graphically extrapolated failure coordinates of T33 and T31 (Appendix E, Table 36). Knowing the location of the break, the author, assuming the lateral and compressive forces acted at the failure position of T31, solved for the failure stress given by the equation (23):

$$S = \frac{(M)(c)}{I} + \frac{P}{A}$$

where: S = failure stress, p.s.i.

M = moment at the break, in. - lbs.

$c = \frac{\text{diameter, i.b. at break, (D), in.}}{2}$

$I = \frac{(\pi)D^4}{64}$, in.^{4} - moment of inertia

P = compressive load, lbs.

$A = \frac{(\pi)D^2}{4}$, in.^{2} - cross-sectional area at the break

$\frac{(M)(c)}{I}$ = modulus of rupture, p.s.i.

$\frac{P}{A}$ = compressive stress, p.s.i.

The failure stresses were calculated at all the breaks in the test trees (Table 5). This concluded the analysis of the field data.

Test Tree	$\frac{(M)(c)}{I}$ (p.s.i.)	$\frac{P}{A}$ (p.s.i.)
1	8868	126
2	7856	54
3	6218	139
4 Top	5520	155
4 Bottom	6082	140
5	6481	172
6	7636	67
7 Top	3817	118
7 Bottom	4451	108
8	11,769	363
9	3211	219

Table 5. Failure Stresses (p.s.i.) at the Breaks

DISCUSSION

One objective of this project was to monitor the movement of the test tree as the cable loadings increased. A major shortcoming was the inability to record the exact position of the stem when failure occurred. To complete the analysis, the author had to extrapolate outside the range of the data collected to determine the original and failure positions. This graphical extrapolation, though not sound statistically, was an acceptable engineering method for determining the "best guess" values of the missing coordinates. A means of making the procedure more acceptable would have been to increase the cable tensions by smaller, more uniform amounts at each loading. The lack of time to conduct the field work, a scheduled three days, necessitated the large loading increments. Also, the mainline drum on the Bantam yarder did not have enough positive control to increase the cable tension uniformly. It is important to note that the total lateral movements, the final cable geometries, the forces acting on the trees at failure, the locations of the breaks at the critical loadings, and the failure stresses occurring at the breaks were calculated using the graphically extrapolated failure coordinates.

The lateral movement at choker height, L, ranged from 4.8 ft. to 17.6 ft. (Table 6) before failure occurred. The largest tree, #4, moved the least, and test tree #2, the smallest, moved the farthest distance laterally. However, this increase in lateral movement was not a smooth function of the decreasing size of the loaded trees. Interference with the limbs and the tops of adjacent trees often took place as noted

Test Tree #	Last Observed Lateral Movement of T31 (ft.)	Extrapolated Lateral Movement of T31 (ft.) at Failure	Diameter o.b., at 5 ft. (in.)
4	2.6[a]	4.6	15.2
8[b]	3.2	5.0	10.4
9[c]	4.0	5.4	11.4
5	4.3	6.3	11.0
7	6.4	7.4	14.8
3	7.6[d]	10.2	13.0
1	7.8	12.9	11.6
6	11.4	13.8	9.5
2	11.6	17.6	8.5

[a] At loading #12

[b] L = 24 ft.

[c] L = 47.3 ft.

[d] At loading #4

Table 6. Lateral Movement (ft.) of the Test Trees at Choker Height.

in Figures 13 through 21. Test tree #2 was able to move a greater lateral distance because its top broke out during loading #4 (Figure 32) and no longer interfered with the tree's motion.

The interference with adjoining tops and branches had a positive effect on the cable tension necessary to move the tree. After the top of tree #2 broke, the cable tension decreased from 3200 lbs. to 1200 lbs. with the compressive load changing from 3853 lbs. to 1407 lbs. The remaining stem finally failed at a cable tension of 1800 lbs. and a compressive force of 2060 lbs. During the loading of test tree #6, the maximum line tension was 4600 lbs. with a corresponding compression load of 5403 lbs. before the branches began to break. With the branches broken, the tree failed at a cable tension of 3000 lbs. and a downward force of 3466 lbs. To eliminate the interaction with other trees, the test tree could have been topped and the surrounding trees felled. This rigging procedure has not been followed during the cable thinning studies conducted at Oregon State. When this interference occurred with trees #2 and #6, the amount of interaction was not measured, but the loadings continued nontheless to demonstrate the effect the surrounding trees had in lending support to the test trees.

Another example of this interference providing additional support was observed with trees #1 and #5. These two trees, similar in size and both rigged at 40 ft., required different tensions to break them. Tree #5, leaning into adjacent tops, required a cable tension of 7800 lbs. and a compressive load of 11,159 lbs. before breaking, compared to the failure cable tension of 5500 lbs. and a compressive force of 8545 lbs for tree #1.

Figure 32. Test tree #2 at loading #4 with its broken top.

The direction of the lateral movement was determined by the geometry of the cable segments. For eight of the nine tests, the trees moved in the general direction of the cable segment with the flatter angle. The angle of the cable segment towards which the tree moved would increase in steepness as the cable tensions rose, while the angle of the other cable segment would decrease. The angles of the cable segments on test tree #9 were nearly equal initially. As the cable was tightened, tree #9 moved perpendicular to the cable, and the angles of both segments decreased as the loadings continued.

Once a tree began moving in a particular direction, it continued to do so despite changes in the direction of the lateral force caused by the cable geometry varying from loading to loading. The compressive load would overcome any effect of the lateral force, and the test tree would bend downwards in the plane of its initial motion.

The failure stresses at the breaks of the test trees were within the ranges of published values (7) with the exception of tree #7. The stresses calculated for the breaks in test tree #7 were low, possibly due to a missed tension reading. The failure tension for the tree was recorded at 7100 pounds, but this particular tension reading was irregular. Another explanation for the low failure stresses could be that the tree had a weakened area, such as a snow break, along its stem (14). Wind damage could be ruled out as some of the other trees would have exhibited low failure stresses if the stand had experienced a severe windstorm.

As listed in Table 4, the breaks occurred in the middle-third sections of the stems, with the exception of tree #9. For the 40 ft. trees, the breaks were located between 16.09 ft. and 26.60 ft. above the ground. Test tree #8, a 24 ft. tree, broke at 9.13 ft. The middle-third section of test tree #9, rigged at a height of 47.25 ft., ranged from 15.75 ft. to 31.50 ft., but the stem broke at 32.44 ft.

Seven of the trees broke along a horizontal plane at the failure height, while trees #4 and #7 broke in two places, exhibiting a characteristic compression failure. The strength of wood in tension and compression along the grain will be different, being much greater in

tension (17). Under loading, a wood beam will first give way at the surface on the compression side and these fibers will lose some of their ability to sustain a load. The adjacent fibers will receive a greater stress, and with this redistribution of stress, the neutral axis will move toward the tension side, shortening the arm of the internal resisting couple, giving a much higher stress in tension. The process will continue until tension failure occurs. The compression failure was the bottom break recorded in the paper.

The compressive loadings at failure for the seven trees rigged at 40 ft. are compared to Pestal's table values (24), Biggs' formula (4), and Euler's design equation (15) (Figure 33). The end conditions are assumed for the case of one end fixed and one end free (a = 4.00 for Biggs and K = 0.25 for Euler). The values published by Pestal are for both ends pinned and have to be reduced by a factor of four before plotting on Figure 33 to match the end conditions assumed in Biggs' and Euler's formulas. The horizontal axis is the diameter at L/2 or the mean diameter used by Pestal and Biggs. The value of D in the Euler equation is the diameter of 2L/3. Assuming a taper of 1 in./10 ft. for the trees tested, D equals D at L/2 minus 0.667 in. The Euler curve is plotted without a safety factor, thus one can see that Pestal and Biggs employ an approximate safety factor of five in their designs for intermediate support trees. Pestal's and Biggs' design methods are for pine and spruce species, not Douglas-fir.

The true Euler equation, with D at 2L/3, is compared with the test results (Table 7 and Figure 34). The modulus of elasticity is

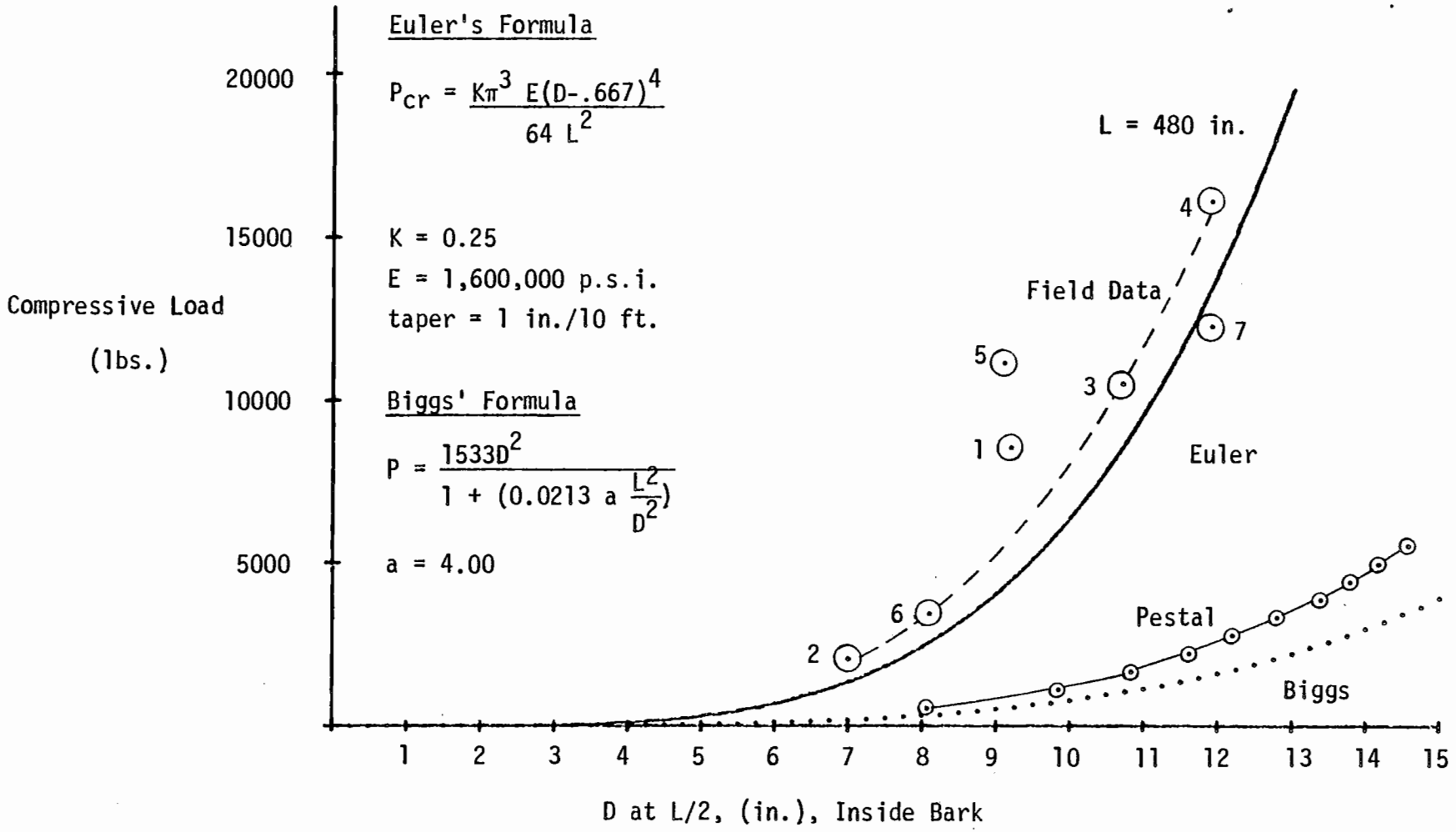

Figure 33. Comparison of the test failure compressive loads With Pestal's, Biggs', and Euler's methods.

Tree #	Dia. at 2L/3 Outside Bark (in.)	Dia. at 2L/3 Inside Bark* (in.)	Length L (in.)	Compressive Load at B2 at Failure (lbs.)	Euler's Critical Load P_{cr} ** (lbs.)
1	9.2	8.6	480	8545	4601
2	7.0	6.6	480	2060	1596
3	10.5	9.8	480	10,494	7758
4	11.5	10.7	480	16,087	11,025
5	9.2	8.6	480	11,159	4601
6	8.2	7.7	480	3466	2957
7	12.1	11.3	480	12,239	13,714
8	9.2	8.6	288	23,580	12,780
9	9.2	8.6	567	13,343	3290

* Diameter inside bark = (0.93 x diameter outside bark) + 0.04

** $P_{cr} = \frac{K(\pi)^3 ED^4}{64(L)^2}$

where: K = 0.25, one end free, one end fixed
E = 1,600,000 p.s.i.
D = diameter inside bark, inches
L = length, inches

Table 7. Comparison of P_{cr} (Euler) and the Test Failure Compressive Loads (lbs.).

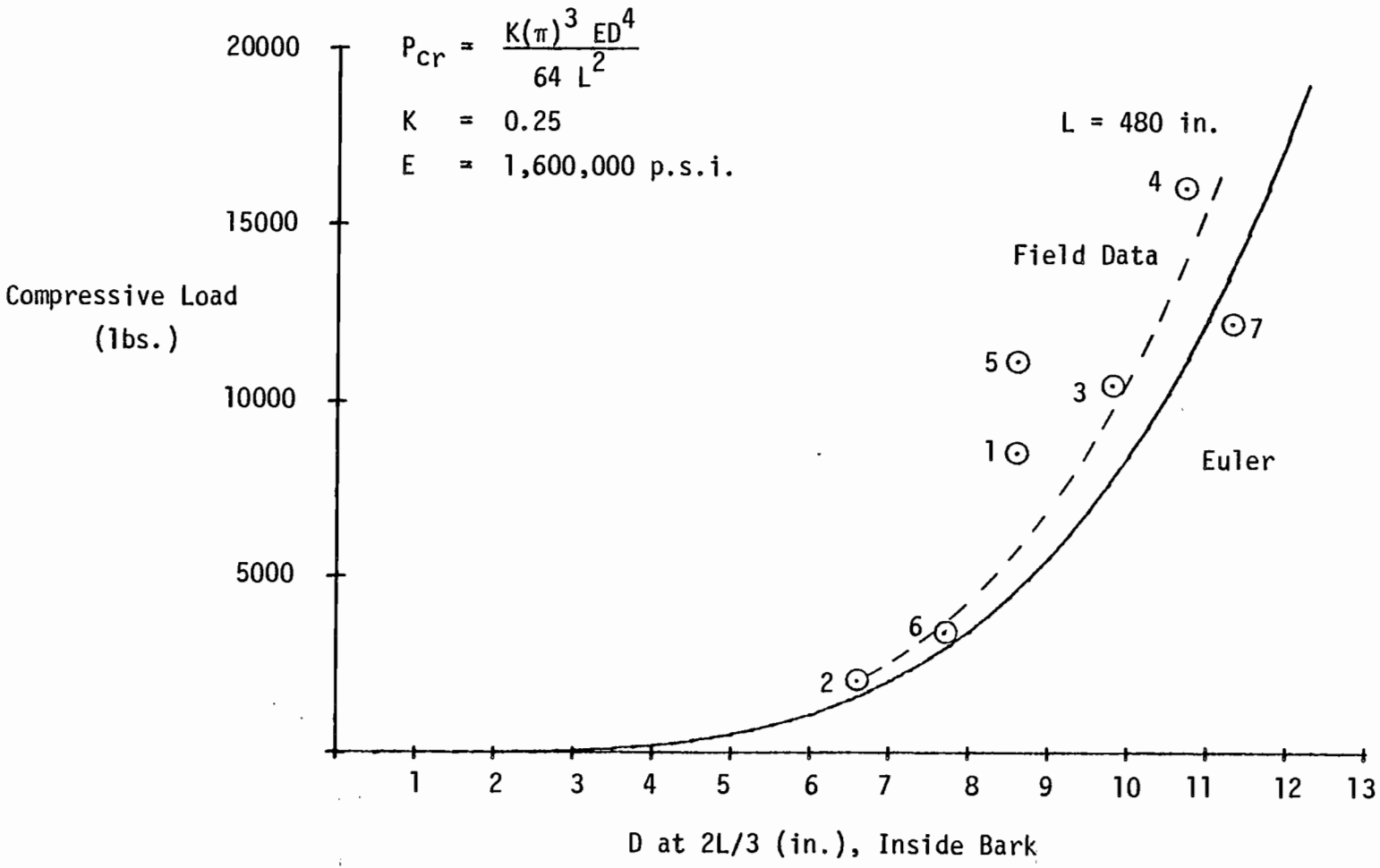

Figure 34. Comparison of the test failure compressive loads with the Euler equation.

assumed to be 1,600,000 p.s.i. for coast Douglas-fir (5). This value will vary from tree to tree, but it was not measured for this study. The end condition constant, K, is equal to 0.25 for the case of one end fixed and one end free. This was not the actual end conditions of some of the trees in the experiment when the surrounding branches provided some resistance to lateral motion.

The comparison between the test values and the theoretical buckling loads were only plotted for a rigging height of 40 ft. Trees #1 and #5, rigged at 40 ft., tree #8, rigged at 24 ft., and tree #9, rigged at 47.25 ft. all had diameters of 8.6 in., i.b., at 2L/3. Euler's formula predicts that the critical loads necessary to fail these trees should be proportional to $1/L^2$. Due to the interference with adjacent tops and limbs, the comparisons between the failure loads for the different rigging heights cannot be justified. Test tree #1 had no interference with surrounding trees and tree #8 barely hit the top of the tree at B3. The ratios for these two trees were:

$$\frac{\text{compressive failure load (\#8)}}{\text{compressive failure load (\#1)}} = \frac{23{,}580 \text{ lbs.}}{8545 \text{ lbs.}} = 2.76$$

$$\frac{(40 \text{ ft.})^2}{(24 \text{ ft.})^2} = \frac{1600}{576} = 2.78$$

Insufficient data was collected to compare statistically the test results with the theoretical curve. Euler's formula underestimated the failure load for every tree, with the exception of tree #7, which was unusual in its response to loading as has already been discussed. The assumption of fixed end conditions at the ground was justified because none of the trees uprooted. Other variables that could influence the

ability of a tree to sustain a compressive load which were not measured include moisture content, modulus of elasticity, tree form, and the presence of knots and other defects.

The Euler formula with K = 0.25, provides a rational basis for design if a safety factor of two or three is employed. More trees should be tested without interference from surrounding trees to verify this. A valuable extension of this project would be a study of the actual loads imposed upon an intermediate support tree rigged in various configurations. An investigation of whether cable logging operations in a given stand of timber could generate the forces capable of breaking the average tree in this stand should be conducted.

SUMMARY

The major objective of this project was to study the ability of second-growth Douglas-fir (Pseudotsuga menziesii (Mirb.) Franco) to sustain compressive loads. These loads were applied to simulate the forces experienced by intermediate support trees utilized in cable logging systems of the Pacific Northwest. The test trees were rigged similar to support trees. They were not topped and the surrounding trees were left standing to represent the conditions present on a thinning show.

A true compressive loading was not applied as the force did not act along the axis of the stem. Except for tree #9, there was always a significant difference between the angles of the two cable segments, B3B2 and B1B2, at the initial set-up. During the cable tightening, the test tree would tend to move in the direction of the flatter cable angle. Once the direction of motion was established, the tree continued its movement along this path. The fact that the lateral force changed direction as the loadings increased did not alter the tree's motion, for the much larger downward compressive force continued to bend the stem in its plane of motion.

A weak point in the experiment was the inability of the Bantam yarder's mainline drum to increase the cable tension in uniform amounts. In several cases, the trees would fail after only two or three loading increments. Small, uniform increases in the cable tension would have lent more credence to the graphical extrapolations used to determine the original and failure locations of the test tree.

The table developed by Pestal (24) and Biggs' formula (4) apply to pine and spruce species and should not be used in the design of Douglas-fir support trees. The experimental compressive loads at failure are compared directly with the Euler formula (15). An end condition constant of 0.25 is assumed, corresponding to one end fixed and one end free. The fixed end condition is a valid assumption as none of the test trees moved noticeably at the base. The top was not completely free because the cable itself may have restricted the stem's motion. The tops and the branches of adjacent trees provided resistance to a tree's motion as evidenced by the decrease in cable tension required to hold the stem at a given displacement once the top or branches broke.

A modulus of elasticity of 1,600,000 p.s.i. was assumed for every test tree. To account for the variablility among the stems, one could have determined the moisture content and the modulus of elasticity of each tree by testing samples in a laboratory. Additional field testing could be done to demonstrate statistically that Euler's equation was an appropriate model for the loading capability of second-growth Douglas-fir. However, the time and the money budgeted for this project limited the number of trees tested.

An extension of this research would be to examine the actual forces acting on support trees during the yarding cycle. One should determine if the logging on a thinning side could possibly generate the forces necessary to fail the average tree in a given stand of timber.

Trees are far from ideal structural members. However, standing or

raised trees will be used by loggers for the sake of expediency and profitability. A safety factor of two or three should be employed when Euler's formula is used in the design of support trees. Pestal's and Biggs' use of a factor of safety of five seems undoubtedly conservative for logging in a stand of second-growth timber.

BIBLIOGRAPHY

BIBLIOGRAPHY

1. Allen, John W. April, 1939. Buckling of wooden beams without lateral support. Oregon State College. Master's Thesis 403. 61 p.

2. Aulerich, D.E. 1975. Smallwood harvesting research at Oregon State University. Loggers Handbook, Vol. XXXV. p. 10-12, 84-88.

3. Beer, Ferdinand P. and E.R. Johnston, Jr. 1962. Vector mechanics for engineers. New York. McGraw-Hill Book Company. 781 p.

4. Biggs, Donald. March, 1973. Cablecrane design studies. Forestry Commission. London, England. 52 p.

5. Biggs, Donald. October, 1976. Personal communication. Department of the Environment. London, England.

6. Donnell, L.H. 1938. On the application of Southwell's method for the analysis of buckling tests. Contributions to the mechanics of solids, dedicated to S. Timoshenko. New York. The MacMillan Company. p. 27-38.

7. Forest Products Laboratory. 1974. Wood handbook: wood as an engineering material. U.S.D.A. Handbook 72. Washington D.C. U.S. Government Printing Office. 356 p.

8. Fons, W.L. and W.Y. Pong. November, 1957. Tree breakage characteristics under static loading ponderosa pine. Technical Report AFSWP-867. California Forest and Range Experiment Station. Forest Service U.S.D.A. Berkeley, California. 51 p.

9. Froehlich, H.A. December, 1977. Personal communication. Associate Professor, Forest Engineering Department, Oregon State University. Corvallis, Oregon.

10. Garratt, George A. 1931. The mechanical properties of wood. New York. John Wiley and Sons, Inc. 276 p.

11. Khan, Faqir Mohammad, John F. Bell, and Alan B. Berg. 1977. Estimating diameter inside bark at various heights in young Douglas-fir trees. Research Note No. 59. Forest Research Laboratory, Oregon State University. Corvallis, Oregon. 2 p.

12. Lundquist, Eugene E. July, 1938. Generalized analysis of experimental observations in problems of elastic stability. National Committee for Aeronautics Technica Note 658. Washington D.C. U.S. Government Printing Office. 13 p.

13. Mergen, Francois. February, 1954. Mechanical aspects of wind-breakage and wind-firmness. Journal of Forestry. 52:119-125.

14. Mergen, Francois and Herbert I. Winer. September, 1952. Compression failures in the boles of living conifers. Journal of Forestry. 50:677-679.

15. Newlin, J.A. and J.M. Gahagan. February, 1930. Tests of large timber columns and presentation of forest products laboratory column formula. U.S.D.A. Technical Bulletin 167. Washington D.C. U.S. Government Printing Office. 43 p.

16. Newlin, J.A. and G.W. Trayer. 1924. Deflection of beams with special reference to shear deformations. Ninth annual report of the National Advisory Committee for Aeronautics. Washington D.C. U.S. Government Printing Office. p. 355-373.

17. Newlin, J.A. and G.W. Trayer. 1924. Form factors of beams subjected to transverse loading only. Ninth annual report of the National Advisory Committee for Aeronautics. Washington D.C. U.S. Government Printing Office. p. 375-393.

18. Newlin, J.A. and G.W. Trayer. 1925. Stresses in wood members subjected to combined column and beam action. Tenth annual report of the National Advisory Committee for Aeronautics. Washington D.C. U.S. Government Printing Office. p. 93-105.

19. Newlin, J.A. and Thomas R.C. Wilson. 1917. Mechanical properties of woods grown in the United States. U.S.D.A. Bulletin 556. Washington D.C. U.S. Government Printing Office. 47 p.

20. Pestal, Ernst. June, 1977. Personal communication. Professor of Forest Engineering, Hochschule fur Bodenkultur. Vienna, Austria.

21. Peters, Penn. Winter, 1977. Aerial logging systems mechanics - class notes. Forest Engineering Department, Oregon State University. Corvallis, Oregon.

22. Pong, W.Y. October, 1956. Tree breakage characteristics under static loading of several hardwood species. Technical Report AFSWP-970. California Forest and Range Experiment Station. Forest Service U.S.D.A. Berkeley, California. 46 p.

23. Timoshenko, S.P. and J.M. Gere. 1972. Mechanics of Materials. New York. D. Van Nostrand Company. 552 p.

24. United Nations. 1972. Symposium on forest operations in mountainous regions. Technical Report TIM/EFC/WP. 1/1. Joint Committee on Forest Working Techniques and Training of Forest Workers. Sponsored by Economic Commission for Europe, Food and Agriculture Organization, and International Labour Organization. pp. 26-33.

APPENDIX A

Side View

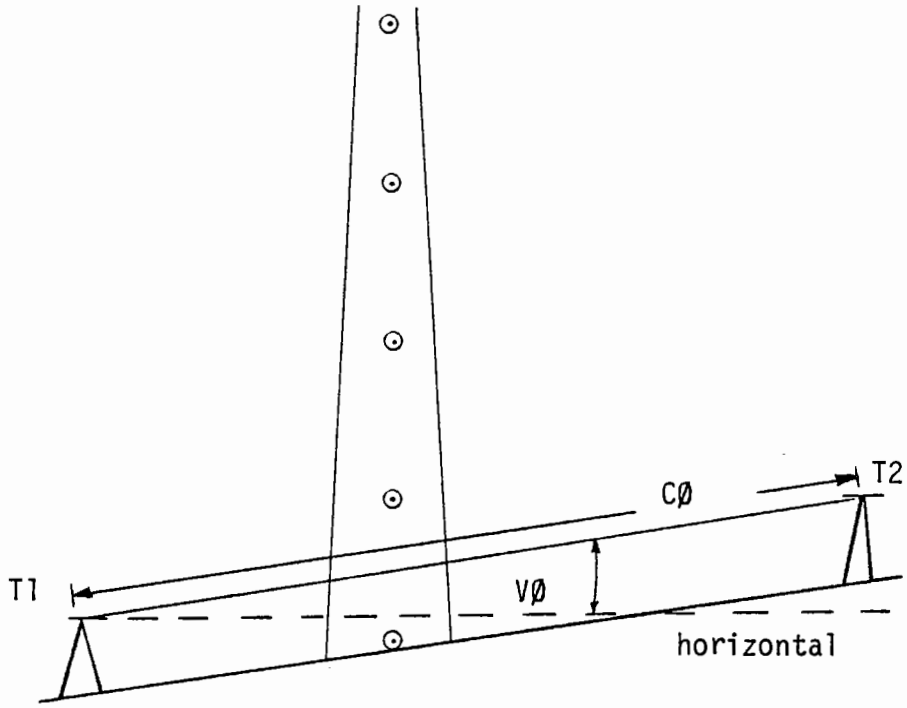

T1, T2 = theodolites

CØ = slope distance (ft.) from T1 to T2

VØ = vertical angle (deg.) from T1 to T2

Note: Coordinates of T1 = (0,0,0)

Figure 35. Readings with the theodolite and the steel tape at cable tightening.

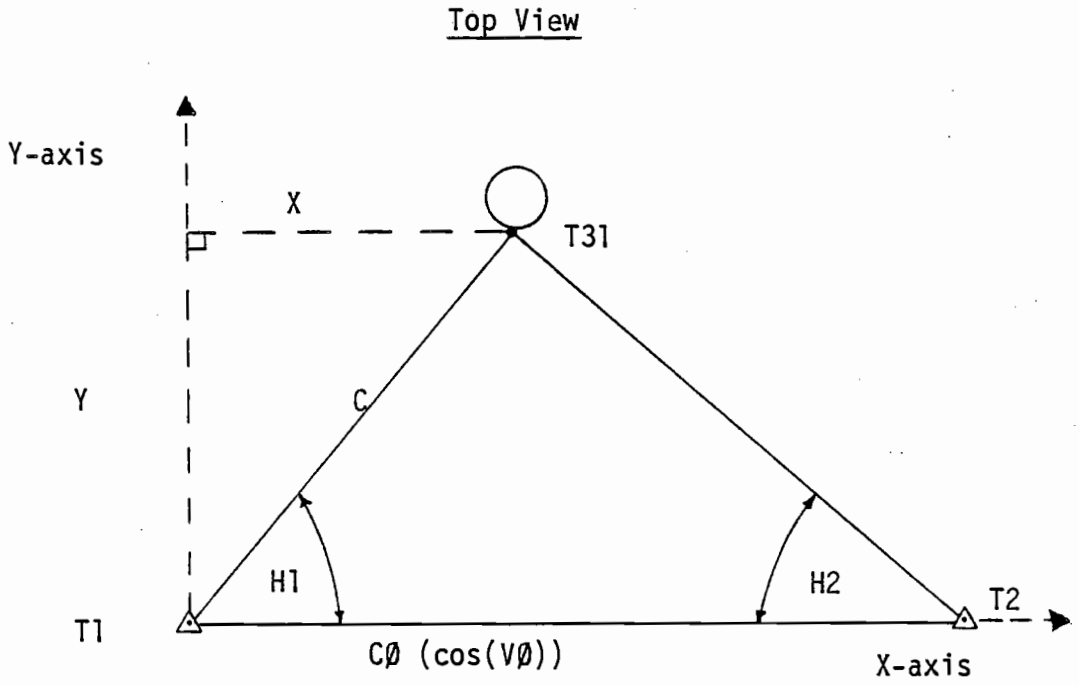

H1, H2 = horizontal angles (deg.) measured in the field

$$C = \frac{C\emptyset\ (\cos(V\emptyset))\ \sin(H2)}{\sin\ (180 - (H1 + H2))}$$

$$X = C\ (\cos\ (H1))$$

$$Y = C\ (\sin\ (H1))$$

Figure 36. Calculation of X and Y coordinates (ft.) for T31.

Side View

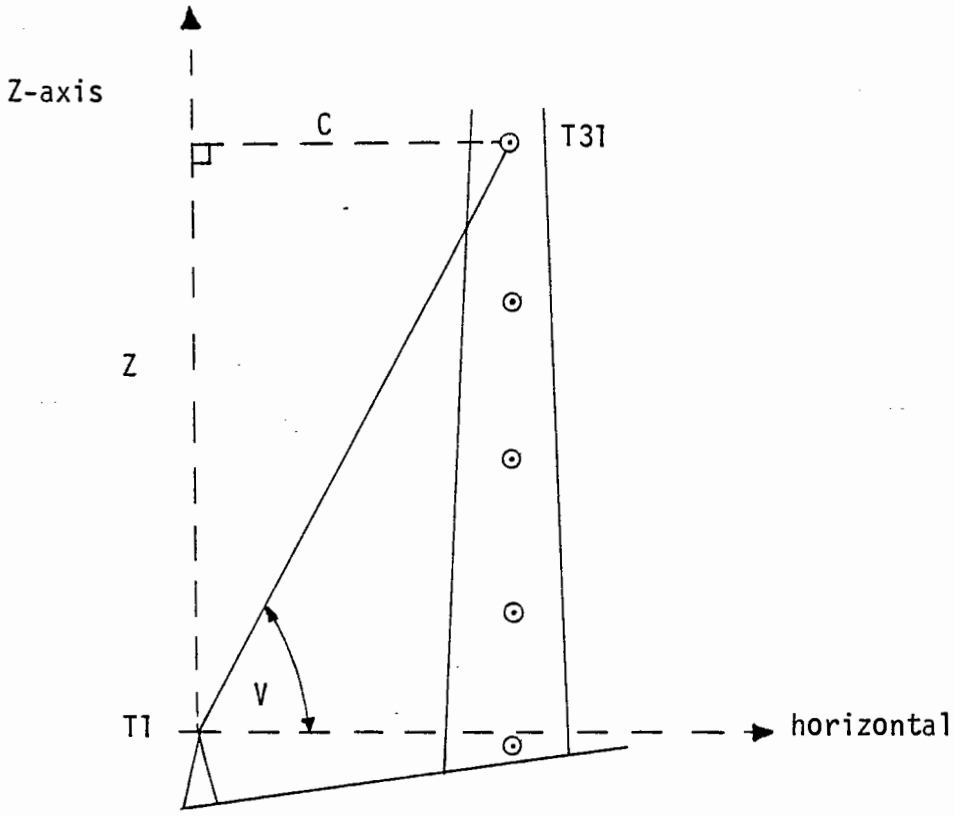

V = vertical angle (deg.) measured from T1

Z = C(tan(V))

Figure 37. Calculation of Z coordinate (ft.) for T31

Top View

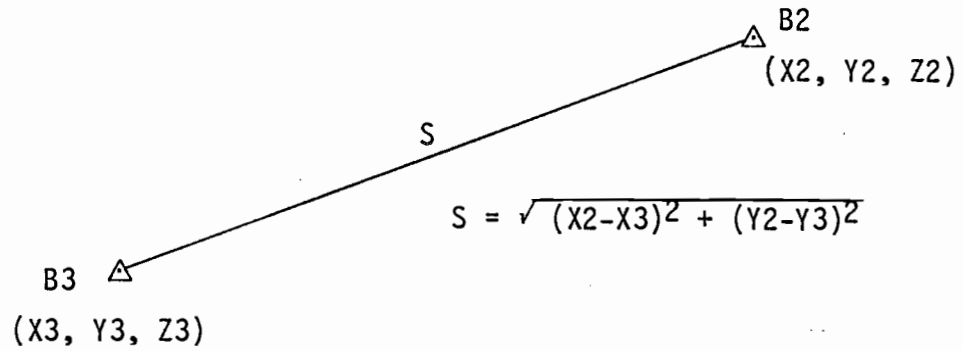

Side View

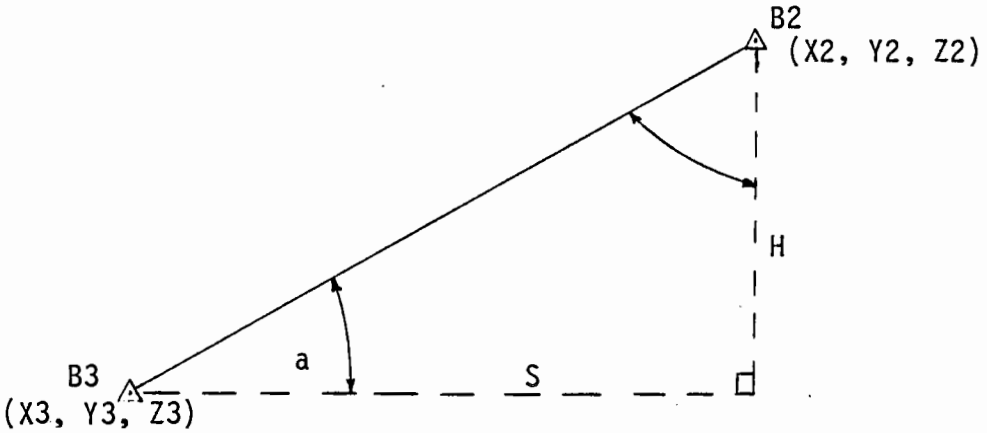

$$a = \tan^{-1} \frac{(H)}{(S)}$$

$$a = \tan^{-1} \frac{(Z2-Z3)}{S}$$

Figure 38. Calculation of the cable angle B3B2 (deg.)

APPENDIX B

Point	Coord. Axis	Position or Loading #							
		Orig-inal*	Tight-ening	1	2	3	4	5	Failure*
	X		0.00						
T1	Y		0.00	DOES	NOT	CHANGE			
	Z		0.00						
	X		30.98						
T2	Y		0.00	DOES	NOT	CHANGE			
	Z		5.39						
	X		27.75						
B1	Y		81.75	DOES	NOT	CHANGE			
	Z		11.31						
	X	25.52	25.52	25.45	25.60	25.64	25.83	25.95	26.82
B2	Y	56.56	57.11	57.70	59.31	59.53	61.19	63.21	69.96
	Z	39.16	38.36	37.78	37.11	36.98	36.19	36.73	36.01
	X		21.37						
B3	Y		35.87	DOES	NOT	CHANGE			
	Z		6.35						
	X	24.92	25.04	25.18	25.37	25.42	25.65	25.88	26.92
T31	Y	55.39	56.36	57.28	59.31	59.66	61.65	63.16	68.14
	Z	41.78	41.78	41.68	41.60	41.52	41.13	40.77	38.23
	X		24.89						
T32	Y		55.91						
	Z		31.97						
	X	24.79	24.79	24.81	24.84	24.83	24.89	24.92	25.15
T33	Y	55.01	55.38	55.62	56.10	56.15	56.55	56.80	57.82
	Z	22.03	22.03	22.04	22.03	22.02	22.00	21.97	21.75
	X		24.83						
T34	Y		55.08						
	Z		12.18						
	X		25.38						
T35	Y		54.72	DOES	NOT	CHANGE			
	Z		2.74						

* Extrapolated

Table 8. Coordinates (ft.) for Test Tree #1.

Point	Coord. Axis	Position or Loading #						
		Original*	Tightening	1	2	3	4	Failure*
T1	X		0.00					
	Y		0.00	DOES	NOT	CHANGE		
	Z		0.00					
T2	X		27.86					
	Y		0.00	DOES	NOT	CHANGE		
	Z		2.24					
B1	X		-20.06	-20.54	-20.28	-19.70	-19.58	
	Y		94.19	95.26	94.44	92.67	92.11	
	Z		4.95	5.19	6.05	7.51	7.85	
B2	X	-0.20	-0.65	-1.92	-3.30	-4.77	-7.76	-11.60
	Y	51.93	52.23	52.89	54.06	55.75	60.40	64.73
	Z	34.90	34.90	34.75	34.56	33.93	32.31	30.80
B3	X		7.89	7.97	7.89	7.85	7.59	
	Y		22.45	21.96	22.00	22.55	22.83	
	Z		2.33	3.09	3.14	3.45	2.93	
T31	X	0.46	-0.04	-1.45	-2.95	-4.60	-7.54	-11.54
	Y	51.63	51.88	52.69	53.91	55.62	59.98	64.43
	Z	38.73	38.73	38.70	38.63	38.14	35.87	34.48
T32	X		-0.02					
	Y		51.82					
	Z		28.88					
T33	X	0.12	-0.02	-0.41	-0.82	-1.22	-2.08	-3.23
	Y	51.78	51.88	52.12	52.50	52.95	54.08	55.23
	Z	18.95	18.95	18.95	18.96	18.92	18.74	18.59
T34	X		-0.29					
	Y		51.91					
	Z		9.08					
T35	X		-0.68					
	Y		51.68	DOES	NOT	CHANGE		
	Z		-0.63					

* Extrapolated

Table 9. Coordinates (ft.) for Test Tree #2.

Point	Coord. Axis	Position or Loading #							
		Orig-inal*	Tight-ening	1	2	3	4	5**	Failure*
	X		0.00		DOES	NOT	CHANGE		
T1	Y		0.00						
	Z		0.00						
	X		65.00						
T2	Y		0.00		DOES	NOT	CHANGE		
	Z		8.88						
	X		57.38						
B1	Y		66.85		DOES	NOT	CHANGE		
	Z		11.13						
	X	41.69	41.69	41.89	42.20	42.44	43.04	43.63	43.34
B2	Y	41.77	42.22	43.54	45.07	45.86	48.61	50.92	50.72
	Z	38.78	38.78	38.64	38.40	38.26	37.51	36.60	37.03
	X		29.86						
B3	Y		27.19		DOES	NOT	CHANGE		
	Z		6.31						
	X	41.53	41.58	41.82	42.16	42.34	42.93		43.33
T31	Y	40.54	41.14	42.59	44.21	45.11	48.02	N/A	50.59
	Z	41.54	41.54	41.51	41.40	41.29	40.67		40.49
	X		42.07						
T32	Y		41.53						
	Z		31.83						
	X	41.27	41.27	41.35	41.44	41.48	41.64		41.73
T33	Y	40.50	40.64	41.03	41.44	41.67	42.33	N/A	42.95
	Z	21.47	21.47	21.48	21.47	21.46	21.42		21.38
	X		41.18						
T34	Y		40.49						
	Z		11.62						
	X		41.09						
T35	Y		40.07		DOES	NOT	CHANGE		
	Z		2.32						

* Extrapolated; ** Tree fails between loadings #4 and #5; breaks while recording angles at #5.

Table 10. Coordinates (ft.) for Test Tree #3.

Point	Coord. Axis	Position or Loading #								
		Orig-inal*	Tight-ening	1	2	3	4	5	6	7
	X		0.00							
T1	Y		0.00	DOES	NOT	CHANGE				
	Z		0.00							
	X		62.24							
T2	Y		0.00	DOES	NOT	CHANGE				
	Z		2.79							
	X		45.98	46.01	46.48	46.67	46.59	46.66	46.67	46.68
B1	Y		5.16	5.02	5.06	5.23	5.29	5.15	5.12	5.12
	Z		3.52	3.53	5.47	6.11	6.25	7.23	8.50	8.51
	X	28.17	28.17	27.96	28.05	28.00	28.15	28.06	28.12	28.23
B2	Y	41.92	41.92	41.64	41.32	41.15	40.48	40.45	40.15	39.56
	Z	32.89	32.89	32.88	32.83	32.82	32.67	32.66	32.65	32.57
	X		6.86	6.81	6.85	6.86	7.61	7.61	7.61	7.64
B3	Y		79.98	79.95	79.85	79.77	78.75	78.75	78.75	78.63
	Z		-0.44	-0.27	-0.16	-0.14	1.18	1.20	1.20	1.17
	X	28.56	28.56	28.30	28.33	28.24	28.30	28.22	28.27	28.36
T31	Y	42.17	42.17	41.86	41.58	41.39	40.71	40.68	40.35	39.75
	Z	35.65	35.65	35.64	35.64	35.64	35.58	35.62	35.58	35.52
	X		28.56							
T32	Y		41.99							
	Z		25.73							
	X	28.64	28.58	28.51	28.52	28.49	28.50	28.48	28.49	28.51
T33	Y	41.76	41.75	41.66	41.59	41.55	41.39	41.39	41.31	41.15
	Z	15.88	15.88	15.88	15.88	15.87	15.86	15.86	15.85	15.85
	X		28.53							
T34	Y		41.44							
	Z		5.90							
	X		28.98							
T35	Y		40.85	DOES	NOT	CHANGE				
	Z		-3.41							

* Extrapolated

Table 11. Coordinates (ft.) for Test Tree #4.

Point	Coord. Axis	Position or Loading #								
		Original*	Tightening	8**	9	10	11**	12	13	Failure*
T1	X		0.00	0.00						
	Y		0.00	0.00	DOES	NOT	CHANGE			
	Z		0.00	0.00						
T2	X		62.24	62.24						
	Y		0.00	0.00	DOES	NOT	CHANGE			
	Z		2.79	2.79						
B1	X		45.98	45.56	45.59	45.32	45.79	45.32	45.32	
	Y		5.16	5.14	5.06	5.24	5.09	5.00	4.98	
	Z		3.52	2.40	2.58	2.70	2.54	2.58	2.59	
B2	X	28.17	28.17	27.61	27.26	27.01	28.98	29.51		29.97
	Y	41.92	41.92	41.42	41.05	40.82	41.03	39.38	N/A	37.37
	Z	32.89	32.89	32.69	32.64	32.58	32.75	32.27		31.39
B3	X		6.86	7.60	7.55	7.51	22.26	22.40	22.59	
	Y		79.98	78.83	78.74	78.70	59.46	59.33	59.08	
	Z		-0.44	1.22	1.27	1.27	3.61	3.62	3.50	
T31	X	28.56	28.56	27.85	27.43	27.15	28.80	29.68		30.56
	Y	42.17	42.17	41.62	41.21	40.98	41.09	39.85	N/A	38.07
	Z	35.65	35.65	35.61	35.60	35.59	35.24	35.17		34.80
T32	X		28.56							
	Y		41.99							
	Z		25.73							
T33	X	28.64	28.58	28.38	28.27	28.20	28.73	28.66	28.95	28.97
	Y	41.76	41.75	41.61	41.52	41.47	41.58	40.81	40.39	40.21
	Z	15.88	15.88	15.87	15.87	15.86	15.87	15.69	15.64	15.62
T34	X		28.53							
	Y		41.44							
	Z		5.90							
T35	X		28.98	28.98						
	Y		40.85	40.85	DOES	NOT	CHANGE			
	Z		-3.41	-3.41						

* Extrapolated; ** Change block position

Table 12. Coordinates (ft.) for Test Tree #4. (cont.)

Point	Coord. Axis	Position or Loading #				
		Original*	Tightening	1	2	Failure*
T1	X		0.00			
	Y		0.00	DOES NOT CHANGE		
	Z		0.00			
T2	X		43.20			
	Y		0.00	DOES NOT CHANGE		
	Z		0.16			
B1	X		4.98	5.07	5.11	
	Y		70.89	70.82	70.65	
	Z		-7.31	-7.21	-7.24	
B2	X	7.89	8.69	9.86	11.25	12.54
	Y	38.76	38.76	38.30	37.03	35.66
	Z	28.54	28.54	28.37	27.98	27.79
B3	X		13.59	13.42	13.57	
	Y		9.21	10.18	10.15	
	Z		-0.96	0.33	0.43	
T31	X	7.18	8.23	9.57	11.10	12.53
	Y	38.48	38.48	37.92	36.64	35.13
	Z	32.26	32.26	32.13	31.90	31.51
T32	X		7.68			
	Y		38.63			
	Z		22.30			
T33	X	7.10	7.33	7.65	8.01	8.36
	Y	38.80	38.80	38.66	38.32	37.92
	Z	12.35	12.35	12.32	12.28	12.16
T34	X		7.03			
	Y		38.85			
	Z		2.44			
T35	X		6.83			
	Y		38.25			
	Z		-7.22			

* Extrapolated

Table 13. Coordinates (ft.) for Test Tree #5.

Point	Coord. Axis	Position or Loading #							
		Original*	Tightening	1	2	3	4	5	Failure*
	X		0.00						
T1	Y		0.00	DOES	NOT	CHANGE			
	Z		0.00						
	X		63.00						
T2	Y		0.00	DOES	NOT	CHANGE			
	Z		-9.30						
	X		9.67	9.64	9.69	9.77	10.02	9.80	
B1	Y		81.93	82.06	82.08	82.12	81.89	82.39	
	Z		7.68	7.98	8.10	8.18	8.23	8.11	
	X	24.49	24.29	24.11	23.87	23.62	23.37	21.98	21.34
B2	Y	41.84	42.19	42.90	44.24	45.97	48.64	52.03	54.04
	Z	33.60	33.60	33.63	33.29	32.95	32.66	31.55	31.00
	X		37.78	37.46	37.53	37.44	37.46	37.46	
B3	Y		1.06	1.05	1.41	1.50	1.59	1.67	
	Z		-6.20	-6.00	-5.41	-5.39	-5.54	-5.68	
	X	24.62	24.34	24.13	23.86	23.61	23.38	21.93	21.27
T31	Y	40.87	41.35	42.12	43.62	45.50	48.29	51.91	54.27
	Z	37.24	37.24	37.27	37.24	37.11	36.67	35.62	35.24
	X		24.10						
T32	Y		41.32						
	Z		27.34						
	X	23.98	23.90	23.84	23.75	23.67	23.64	23.29	23.26
T33	Y	41.35	41.51	41.70	42.12	42.64	43.33	44.21	44.80
	Z	17.37	17.37	17.37	17.40	17.41	17.39	17.30	17.23
	X		23.64						
T34	Y		41.81						
	Z		7.58						
	X		23.34						
T35	Y		42.14	DOES	NOT	CHANGE			
	Z		-2.50						

* Extrapolated

Table 14. Coordinates (ft.) for Test Tree #6.

Point	Coord. Axis	Position or Loading #					
		Orig-inal*	Tight-ening	1	2	3	Failure*
T1	X		0.00				
	Y		0.00	DOES	NOT	CHANGE	
	Z		0.00				
T2	X		62.99				
	Y		0.00	DOES	NOT	CHANGE	
	Z		0.84				
B1	X		32.43	32.44	32.48	32.49	
	Y		16.32	16.18	16.12	16.04	
	Z		0.15	0.70	1.21	1.21	
B2	X	27.93	27.93	27.67	27.34	27.13	26.98
	Y	35.26	35.01	33.60	30.99	29.53	28.86
	Z	29.68	29.68	28.92	28.28	27.98	27.83
B3	X		23.39	23.55	23.47	23.41	
	Y		47.43	46.93	46.39	46.10	
	Z		-0.69	0.91	0.91	0.77	
T31	X	28.32	28.29	27.90	27.44	27.05	26.77
	Y	35.29	35.14	33.67	30.82	29.04	28.09
	Z	32.38	32.38	32.20	31.74	31.19	31.03
T32	X		28.46				
	Y		35.43				
	Z		22.57				
T33	X	28.58	28.58	28.51	28.43	28.40	28.39
	Y	35.80	35.77	35.38	34.67	34.37	34.22
	Z	12.61	12.61	12.56	12.44	12.37	12.32
T34	X		28.64				
	Y		36.17				
	Z		2.60				
T35	X		28.80				
	Y		36.56	DOES	NOT	CHANGE	
	Z		-7.05				

* Extrapolated

Table 15. Coordinates (ft.) for Test Tree #7.

Point	Coord. Axis	Position or Loading #					
		Original*	Tightening	1	2	3	Failure*
T1	X		0.00				
	Y		0.00	DOES NOT CHANGE			
	Z		0.00				
T2	X		81.02				
	Y		0.00	DOES NOT CHANGE			
	Z		6.71				
B1	X		66.86	66.97	66.90	66.85	
	Y		43.20	43.24	43.23	43.24	
	Z		9.40	9.34	9.40	9.53	
B2	X	61.07	60.92	60.34	59.81	58.76	57.42
	Y	41.35	41.35	41.36	41.34	41.31	41.20
	Z	23.26	23.26	23.22	23.18	23.03	22.76
B3	X		47.09	47.06	47.05	47.34	
	Y		38.65	38.66	38.66	38.89	
	Z		5.51	5.56	5.58	6.69	
T31	X	61.07	60.69	59.97	59.28	57.97	56.12
	Y	41.71	41.71	41.68	41.65	41.63	41.16
	Z	27.41	27.41	27.40	27.35	27.19	26.56
T32	X		60.67				
	Y		41.47				
	Z		21.47				
T33	X	60.74	60.65	60.41	60.18	59.80	59.44
	Y	41.27	41.27	41.29	41.30	41.33	41.40
	Z	15.42	15.42	15.40	15.39	15.35	15.32
T34	X		60.49				
	Y		41.05				
	Z		9.47				
T35	X		60.11				
	Y		40.72	DOES NOT CHANGE			
	Z		3.95				

* Extrapolated

Table 16. Coordinates (ft.) for Test Tree #8.

Point	Coord. Axis	Position or Loading #						
		Original*	Tightening	1	2	3	4	Failure*
T1	X		0.00	DOES NOT CHANGE				
	Y		0.00					
	Z		0.00					
T2	X		32.78	DOES NOT CHANGE				
	Y		0.00					
	Z		4.75					
B1	X		14.69	14.81	14.95	15.03	15.19	
	Y		21.95	22.03	22.09	22.16	22.23	
	Z		0.55	0.84	0.87	1.05	1.12	
B2	X	10.74	11.04	11.44	11.80	13.05	14.23	15.49
	Y	55.99	55.99	55.82	55.67	55.76	55.47	55.44
	Z	39.81	39.81	39.62	39.47	39.21	38.87	38.61
B3	X		7.55	7.54	7.58	8.06	8.28	
	Y		89.94	90.28	90.25	89.62	89.55	
	Z		2.76	3.30	3.35	4.27	4.27	
T31	X	10.30	10.58	11.05	11.48	12.84	14.20	15.60
	Y	56.40	56.07	55.82	55.63	55.59	55.45	55.30
	Z	43.47	43.47	43.35	43.21	43.10	43.03	42.92
T32	X		10.39					
	Y		56.14					
	Z		31.52					
T33	X	10.10	10.15	10.24	10.32	10.57	10.72	11.01
	Y	56.11	56.11	56.07	56.05	56.11	56.10	56.11
	Z	19.71	19.71	19.70	19.70	19.69	19.68	19.67
T34	X		10.13					
	Y		56.01					
	Z		7.92					
T35	X		10.46	DOES NOT CHANGE				
	Y		55.81					
	Z		-3.52					

* Extrapolated

Table 17. Coordinates (ft.) for Test Tree #9.

APPENDIX C

Loading	Cable Tension (lbs.)	Coordinate Axis		
		X-Lateral (lbs.)	Y-Lateral (lbs.)	Z-Compressive (lbs.)
Tight-ening	1000	-46	122	-1566
1	1700	-71	177	-2644
2	2700	-125	141	-4168
3	3000	-142	137	-4624
4	3500	-188	-25	-5345
5	3900	-210	-298	-6026
Failure	5500	-472	-1752	-8545

Table 18. Forces (lbs.) Acting at B2 for Test Tree #1.

Loading	Cable Tension (lbs.)	Coordinate Axis		
		X-Lateral (lbs.)	Y-Lateral (lbs.)	Z-Compressive (lbs.)
Tight-ening	300	-49	30	-380
1	1100	-133	98	-1360
2	2100	-174	167	-2572
3	3200	-136	202	-3853
4	1200	28	11	-1407
Failure	1800	249	-54	-2060

Table 19. Forces (lbs.) Acting at B2 for Test Tree #2.

Loading	Cable Tension (lbs.)	Coordinate Axis		
		X-Lateral (lbs.)	Y-Lateral (lbs.)	Z-Compressive (lbs.)
Tight-ening	900	69	192	-1394
1	2800	223	464	-4334
2	4500	362	499	-6951
3	5000	387	417	-7713
4	5200	411	-79	-7953
5	4900	387	-483	-7409
Failure*	6900	614	-649	-10,494

* Failure load was attained between loadings #4 and #5. Tree failed while reading angles at #5.

Table 20. Forces (lbs.) Acting at B2 for Test Tree #3.

Loading	Cable Tension (lbs.)	Coordinate Axis		
		X-Lateral (lbs.)	Y-Lateral (lbs.)	Z-Compressive (lbs.)
Tight-ening	1700	-58	-64	-2025
1	4800	-127	-146	-5700
2	6600	-65	-257	-7645
3	8500	4	-326	-9776
4	11,900	42	-289	-13,573
5	13,000	153	-412	-14,616
6	14,000	261	-531	-15,460
7	15,700	344	-464	-17,333
8	8000	-189	-75	-9558
9	12,000	-108	-21	-14,288
10	13,900	-27	56	-16,548
11	2000	291	-392	-2871
12	5900	760	-915	-8386
13	9500	N/A*	N/A*	N/A*
Failure	11,500	1489	-1186	-16,087

*Do not know the location of B2.

Table 21. Forces (lbs.) Acting at B2 for Test Tree #4.

Loading	Cable Tension (lbs.)	Coordinate Axis		
		X-Lateral (lbs.)	Y-Lateral (lbs.)	Z-Compressive (lbs.)
Tight-ening	1800	72	-68	-2600
1	3800	-36	-129	-5463
2	6000	-388	-72	-8592
Failure	7800	-943	134	-11,159

Table 22. Forces (lbs.) Acting at B2 for Test Tree #5.

Loading	Cable Tension (lbs.)	Coordinate Axis		
		X-Lateral (lbs.)	Y-Lateral (lbs.)	Z-Compressive (lbs.)
Tight-ening	1100	-72	111	-1319
1	2200	-153	202	-2626
2	3500	-236	255	-4135
3	4600	-332	227	-5403
4	2700	-220	29	-3178
5	2500	-156	-65	-2899
Failure	3000	-172	-157	-3466

Table 23. Forces (lbs.) Acting at B2 for Test Tree #6.

Loading	Cable Tension (lbs.)	Coordinate Axis		
		X-Lateral (lbs.)	Y-Lateral (lbs.)	Z-Compressive (lbs.)
Tight-ening	400	-4	-62	-702
1	3300	35	-310	-5734
2	6100	255	71	-10,550
3	6800	409	500	-11,746
Failure	7100	518	762	-12,239

Table 24. Forces (lbs.) Acting at B2 for Test Tree #7.

Loading	Cable Tension (lbs.)	Coordinate Axis		
		X-Lateral (lbs.)	Y-Lateral (lbs.)	Z-Compressive (lbs.)
Tight-ening	1900	-417	5	3221
1	5600	-945	3	-9458
2	9000	-1153	-11	-15,175
3	11,200	-660	13	-18,649
Failure	14,300	689	54	-23,580

Table 25. Forces (lbs.) Acting at B2 for Test Tree #8.

Loading	Cable Tension (lbs.)	Coordinate Axis		
		X-Lateral (lbs.)	Y-Lateral (lbs.)	Z-Compressive (lbs.)
Tightening	900	1	18	-1340
1	2100	-26	64	-3099
2	3100	-70	106	-4566
3	5500	-347	176	-8054
4	7400	-758	264	-10,787
Failure	9200	-1411	312	-13,343

Table 26. Forces (lbs.) Acting at B2 for Test Tree #9.

APPENDIX D

Loading	B3 to B2 (Deg.)	B1 to B2 (Deg.)
Tightening	55.9 (S1 = 57.5)*	47.6 (S2 = 48.3)*
1	54.8	47.6
2	52.2	48.9
3	51.9	50.0
4	49.2	50.3
5	47.6	53.8
Failure	40.7	64.4

* S1 and S2 were measured with a clinometer.

Table 27. Cable Angles (deg.) During the Loading of Test Tree #1.

Loading	B3 to B2 (Deg.)	B1 to B2 (Deg.)
Tightening	46.4 (S1 = 45.0)*	32.9 (S2 = 33.0)*
1	44.3	32.6
2	42.8	33.1
3	40.6	33.6
4	35.9	35.9
Failure	31.2	38.8

*S1 and S2 were measured with a clinometer.

Table 28. Cable Angles (deg.) During the Loading of Test Tree #2.

Loading	B3 to B2 (Deg.)	B1 to B2 (Deg.)
Tightening	59.5 (S1 = 60.0)*	43.4 (S2 = 44.0)*
1	57.9	44.5
2	55.9	45.8
3	54.8	46.5
4	51.1	48.7
5	47.8	50.4
Failure	48.6	50.5

* S1 and S2 were measured with a clinometer.

Table 29. Cable Angles (deg.) During the Loading of Test Tree #3.

Loading	B3 to B2 (Deg.)	B1 to B2 (Deg.)
Tightening	37.4 (S1 = 38.0)*	35.7 (S2 = 36.0)*
1	37.1	35.7
2	36.9	33.9
3	36.8	33.4
4	35.9	33.6
5	35.9	32.5
6	35.7	31.3
7	35.4	31.6
8**	36.6	36.8
9	36.4	36.7
10	36.3	36.7
11**	56.1	37.3
12	53.5	38.1
13	N/A***	N/A***
Failure	50.6	38.8

*S1 and S2 were measured with a clinometer.

**Change block position.

***Do not know the location of B2.

Table 30. Cable Angles (deg.) During the Loading of Test Tree #4.

Loading	B3 to B2 (Deg.)	B1 to B2 (Deg.)
Tightening	44.6 (S1 = 46.0)*	47.9 (S2 = 49.0)*
1	44.7	47.3
2	45.6	45.9
Failure	47.0	44.4

*S1 and S2 were measured with a clinometer.

Table 31. Cable Angles (deg.) During the Loading of Test Tree #5.

Loading	B3 to B2 (Deg.)	B1 to B2 (Deg.)
Tightening	42.6 (S1 = 43.0)*	31.5 (S2 = 32.0)*
1	42.1	31.6
2	40.7	31.9
3	39.5	32.6
4	37.9	34.3
5	35.2	35.6
Failure	33.8	36.8

*S1 and S2 were measured with a clinometer.

Table 32. Cable Angles (deg.) During the Loading of Test Tree #6.

Loading	B3 to B2 (Deg.)	B1 to B2 (Deg.)
Tightening	66.5 (S1 = 67.0)*	56.9 (S2 = 57.0)*
1	63.5	57.4
2	59.9	59.8
3	58.0	61.5
Failure	56.9	62.3

* S1 and S2 were measured with a clinometer.

Table 33. Cable Angles (deg.) During the Loading of Test Tree #7.

Loading	B3 to B2 (Deg.)	B1 to B2 (Deg.)
Tightening	51.6 (S1 = 52.0)*	65.8 (S2 = 68.0)*
1	52.5	63.6
2	53.5	62.0
3	54.4	58.4
Failure	57.2	53.9

*S1 and S2 were measured with a clinometer.

Table 34. Cable Angles (deg.) During the Loading of Test Tree #8.

Loading	B3 to B2 (Deg.)	B1 to B2 (Deg.
Tightening	47.3 (S1 = 47.0)	48.9 (S2 = 49.0)
1	46.3	48.8
2	46.0	48.9
3	45.6	48.6
4	45.0	48.6
Failure	44.6	48.5

* S1 and S2 were measured with a clinometer.

Table 35. Cable Angles (deg.) During the Loading of Test Tree #9.

APPENDIX E

Test Tree #	Coordinate Axis		
	X-Axis	Y-Axis	Z-Axis
1	25.19	57.26	18.30
2	-3.38	55.40	18.88
3	42.29	45.63	28.08
4 (Top)	29.17	39.94	18.07
4 (Bottom)	28.97	40.35	11.48
5	8.39	37.90	12.30
6	23.28	44.22	12.93
7 (Top)	28.02	32.81	16.62
7 (Bottom)	28.43	34.45	10.38
8	59.61	41.23	12.45
9	12.73	55.81	28.40

Table 36. Coordinates (ft.) of the Breaks at Failure.